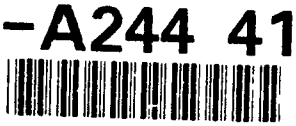

NAVSWC TR 91-178

NOTES ON THE CAUSE OF PARACHUTE CRITICAL VELOCITY

BY WILLIAM P. LUDTKE

UNDERWATER SYSTEMS DEPARTMENT

25 JUNE 1991

NAVAL SURFACE WARFARE CENTER

Dahlgren, Virginia 22448-5000 • Silver Spring, Maryland 20903-5000

FOREWORD

The author presents a new approach to the subject of parachute critical velocity. Aspects of the observed performance of critical parachutes in the field are theoretically developed in the analysis. In addition, the effects of the mass flow ratio on parachute stability, drag coefficient and inflation dynamics are offered.

Approved by:

C. A. Kalivretenos

C. A. KALIVRETENOS, Deputy Head
Underwater Systems Department

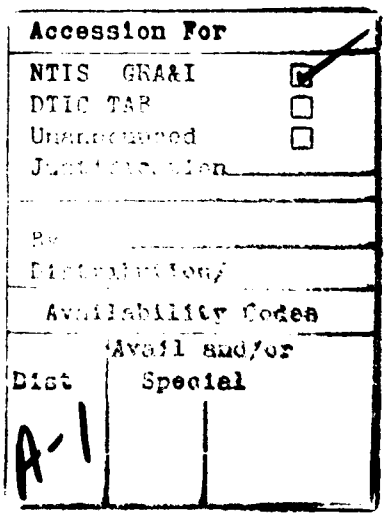

ABSTRACT

This report discusses how the critical velocity of parachutes depends upon the rate of outflow through the canopy surface and the rate of inflow through the canopy mouth. The analysis indicates that the mass flow rate ratio, M', is demonstrated to be the theoretical key to the critical velocity of parachutes. All other observed effects modify the onset of critical velocity. The effects of M' and altitude on inflation reference time, parachute stability, drag coefficient, and inflation rate are also discussed.

CONTENTS

ILLUSTRATIONS

ILLUSTRATIONS (Cont.)

TABLES

INTRODUCTION

Parachutes have a property known as critical velocity where the canopy fails to fully inflate at deployment. Critical velocity is not really understood although some of the effects that modify the onset of critical velocity have been observed. Canopy rate of airflow, altitude, suspension line length, number of gores in the canopy, canopy gore shape and cut, and parachute diameter are all known factors that affect critical velocity.

The key to the solution of this problem came from observation of a critical parachute under test in a wind tunnel. Below the critical velocity, the parachute was fully and satisfactorily inflated. At the critical condition the canopy suddenly collapsed. The inflated canopy actually lost volume due to an increase in velocity. This signaled that the rate of outflow through the canopy surface exceeded the rate of inflow through the canopy mouth and was a function of velocity. The analysis indicates that the mass flow rate ratio, M', is the key element of critical velocity and is shown to theoretically illustrate the described effects. All other observed effects modify the onset of critical velocity.

APPROACH

CRITICAL VELOCITY EFFECTS

One of the more exotic properties of parachutes is the failure to fully inflate during deployment. The critical deployment velocity is the lowest velocity at which the parachute does not fully inflate. Deployment at higher than critical velocity results in a partial inflation of the canopy.

Some of the known phenomena that affect parachute inflation criticality are:

1. Critical velocity is affected by the length of the suspension lines. Increasing the suspension line length raises the critical velocity.

2. Critical velocity is also affected by the number of canopy gores. Increasing the number of gores raises the critical velocity.

3. The rate of airflow through the canopy surface area, and the distribution of the rate of airflow. The rate of airflow for solid cloth parachutes is also affected by whether the gores are block cut or bias cut.

4. The shape of the canopy gore. Figure 1 is a comparison between a triangular gore design and a gore shaped to provide a minimum stress condition and illustrates how gore surface area can be modified.

5. The effect of increasing the deployment altitude is to raise the critical velocity.

6. Imporous parachute canopies always inflate.

7. Critical velocity is a function of parachute diameter.

Theoretical explanations for the above effects have been derived in the several sections of this report. Consider the parachute to consist of two main components: the canopy which produces the aerodynamic forces, and the suspension lines which transmit the aerodynamic force to the payload. The suspension lines are usually connected to the payload in an assembly which result in a steady-state cone angle, β_o, as in Figure 2. The suspension lines are joined to the canopy at the skirt hem. The balance of forces at this connection is a key to critical velocity analysis.

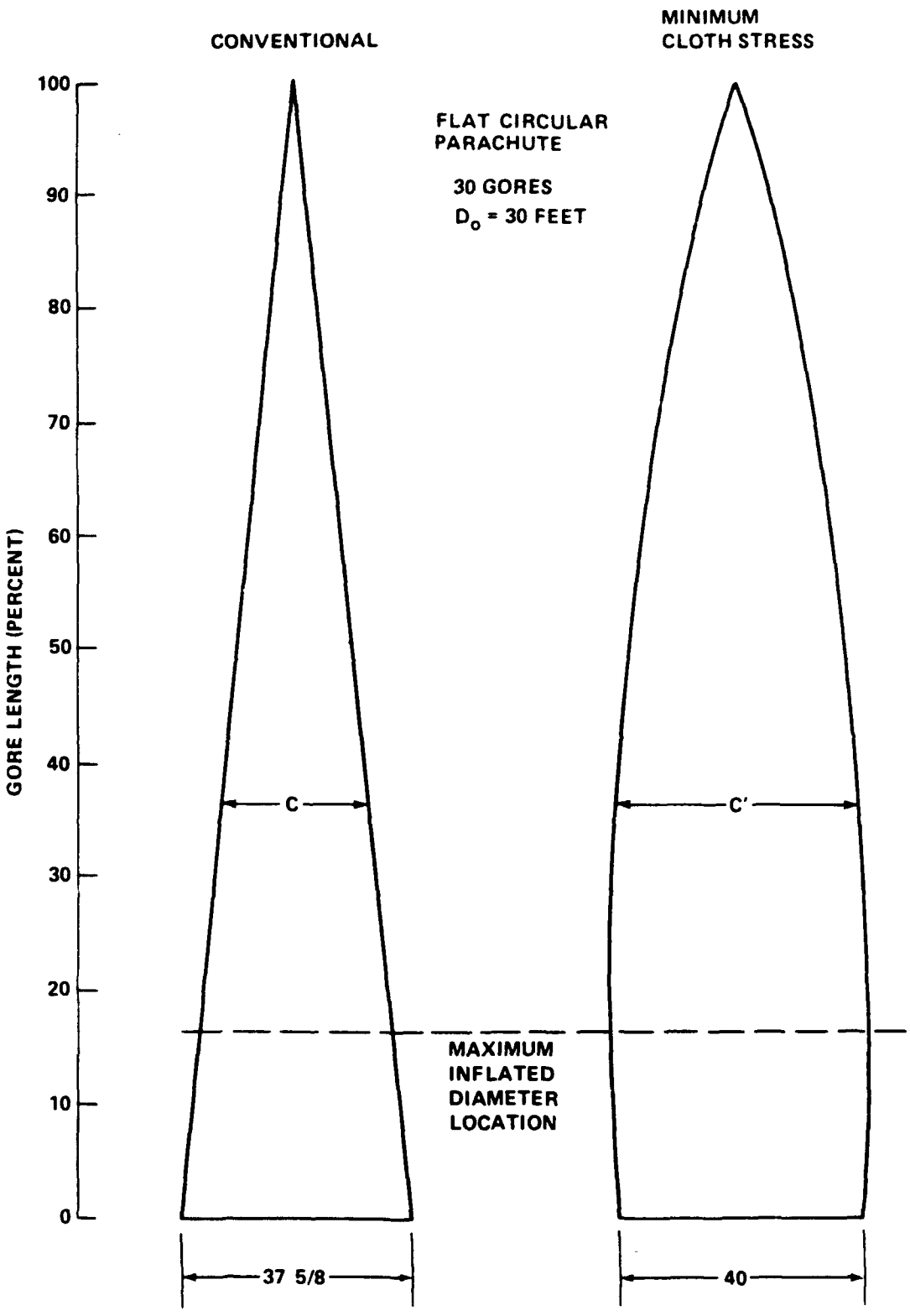

FIGURE 1. COMPARISON OF CONVENTIONAL FLAT CIRCULAR PARACHUTE GORE LAYOUT AND MINIMUM CLOTH STRESS GORE CONFIGURATION

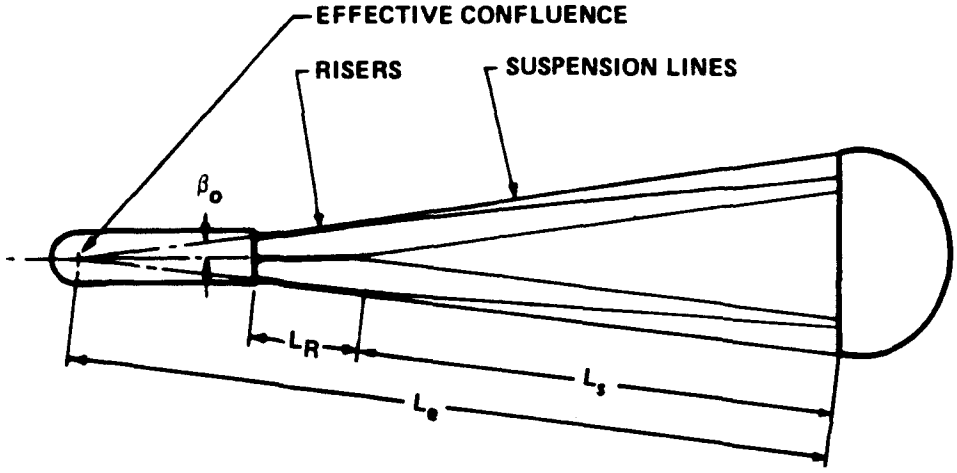

FIGURE 2. EFFECTIVE RIGGING LENGTH WITH MULTIPLE RISER ATTACHMENTS

LENGTH OF SUSPENSION LINES AND NUMBER OF GORES

The effects of suspension line length on the parachute drag coefficient were developed in Reference 1 and are illustrated in Figure 3. As the suspension lines of Figure 4 are lengthened, the radial component of the suspension line force, F_{RL}, is reduced, and the canopy pressure differential, due to the excess cloth in the skirt of a flat parachute, expands the inflated parachute diameter which gives rise to the improved aerodynamic drag of the parachute and increases the canopy steady-state mouth area, A_{MO}. The lengthened suspension lines improve the mouth area throughout the inflation cycle and permit additional mass inflow which results in a higher critical velocity. Shortening of the suspension line length produces the reverse of the conditions cited above. Flaring the canopy mouth improves the inflation characteristics of marginal canopies.

The aerodynamic force generated by the canopy cloth area is transmitted to the canopy main seams. Figure 5 illustrates the relationship between the tangent force in the canopy cloth, F_T, and the canopy radial force, F_{AC}. As the number of gores in the canopy is increased the angle phi approaches zero, see Figure 6. This more effectively converts the aerodynamic cloth tangent force at the main seam into an inflation assisting normal force. Therefore, increasing the number of gores in a canopy improves the critical inflation characteristics and the drag coefficient of the parachute. Reducing the number of gores in a canopy has the opposite effect.

Atmosphere flowing into the canopy mouth is reduced in velocity and is converted into an entrapped air mass at an elevated pressure. The ability of the canopy to entrap sufficient air to completely fill the parachute is the most important element in critical velocity theory. The intensity of the internal pressure depends upon the rate of airflow through the canopy cloth or the ribbon grid and the canopy surface area. Canopies continue to inflate as long as the mass inflow exceeds the mass outflow. Canopy inflation stops at any time that the mass outflow is equal to the mass inflow. Fully inflated parachutes subjected to increasing velocity deflate and collapse after the critical velocity has been reached.

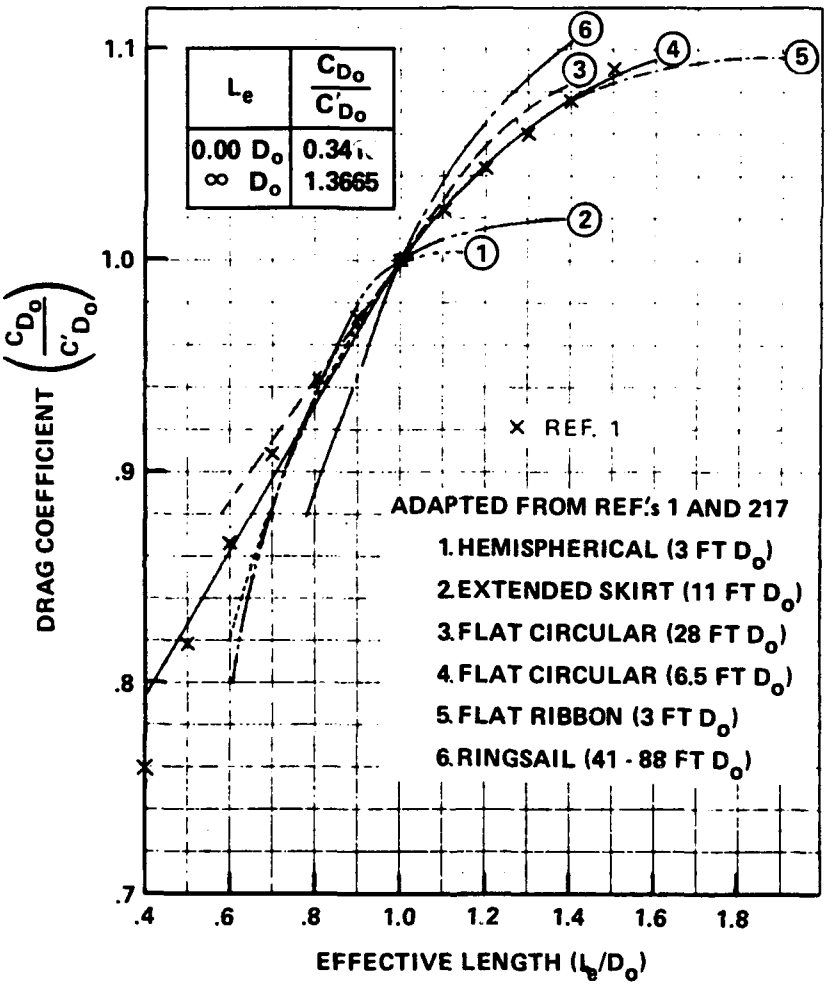

FIGURE 3. EFFECT OF SUSPENSION LINE EFFECTIVE LENGTH ON PARACHUTE DRAG COEFFICIENT

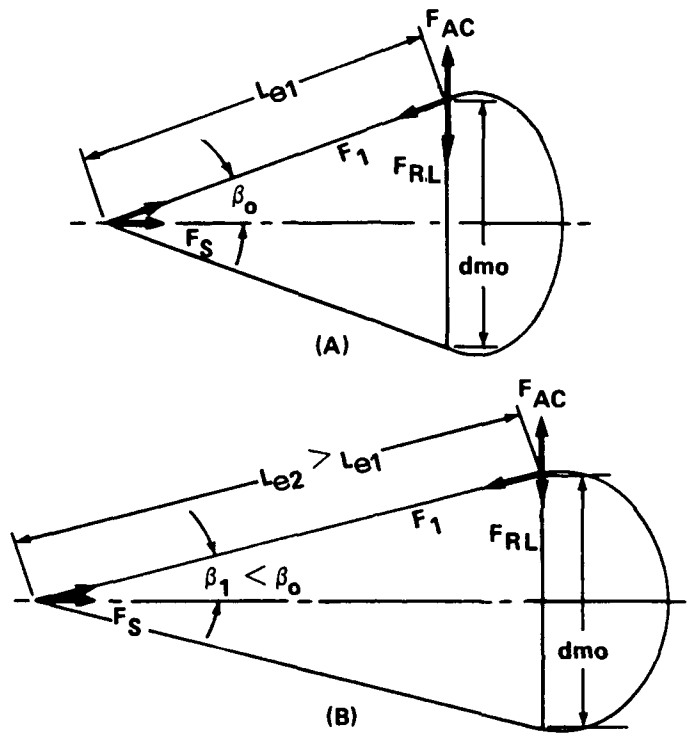

FIGURE 4. EFFECT OF SUSPENSION LINE LENGTH ON THE AERODYNAMIC FORCE BALANCE AT THE SKIRT HEM OF A FLAT TYPE OF PARACHUTE

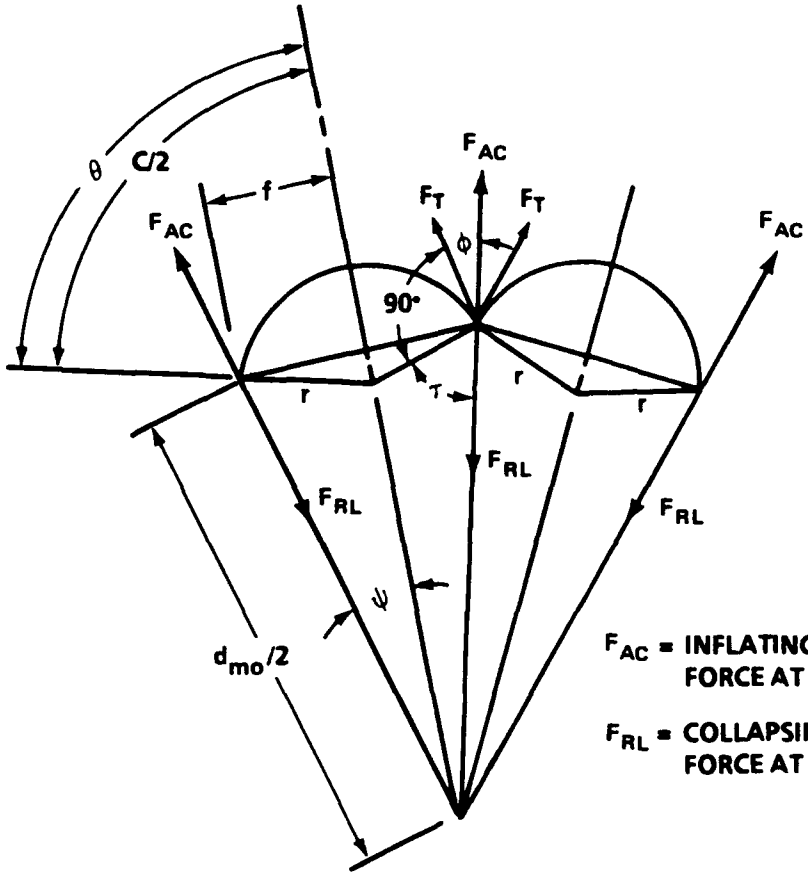

FIGURE 5. CANOPY SKIRT HEM GEOMETRY AND FORCE DISTRIBUTION OF FLAT PARACHUTES IN FULL STEADY-STATE INFLATION

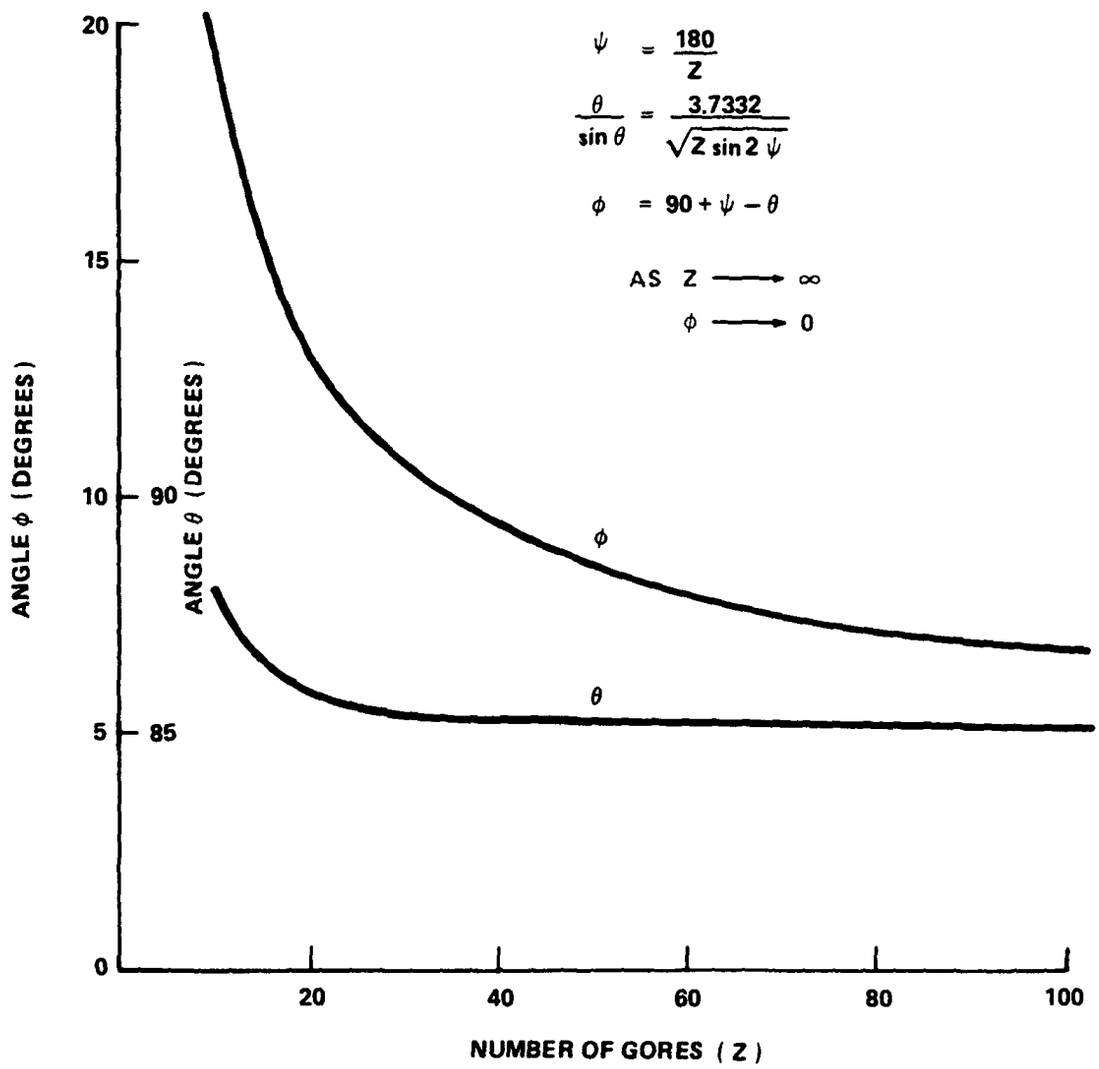

FIGURE 6. EFFECTS OF THE NUMBER OF CANOPY GORES ON THE CLOTH TANGENT FORCE ANGLE ϕ AND GORE BILLOW HALF ANGLE θ

EFFECT OF PARACHUTE DIAMETER ON INFLATION INSTABILITY

Solid cloth parachutes usually use cloths of constant rates of airflow per unit area, and geometrically porous parachutes often use constant porosity over the entire canopy surface. Because of this constancy we tend to envision the flow through the canopy to be constant over the total area. Thus, we confuse total flow rate with flow rate per unit area. The total CFM through the gore is equal to P (CFM/FT^2) times the area of the gore (FT^2), but the flow distribution varies. As the radius of a flat circular parachute proceeds from the center the surface area varies as the square of the radius.

Figure 7 illustrates the distribution of the canopy area and rate of airflow along the radius of a 28 FT, D_o, flat circular canopy. The canopy is divided into concentric rings of one foot width. Each ring's area was normalized by ratioing it to the area of the first ring.

$$R_{at} = \frac{A_R - A_{(R-1)}}{A_{R=1}}$$

$$R_{at} = \frac{\pi R - \pi(R-1)^2}{\pi(1)^2}$$

$$R_{at} = 2R - 1$$

A canopy with a constant cloth flow rate per unit area or geometric porosity has a varying flow rate along the radius due to the increase in area. The canopy airflow in CFM is a minimum in the canopy vent area and a maximum at the canopy skirt hem. As an example, the area of the ring between the R=13 FT and R=14 FT radii is equal to the 84.82 FT^2 area of an R=5.20 FT disc. Critical parachutes partially inflate because the high flow rate per unit of cloth area in the crown area of the canopy lacks sufficient area to produce an outflow that exceeds the inflow. Canopy inflation continues until the outflow is equal to the inflow. At this point the canopy ceases to convert the velocity head of the flow to a pressure head which can proceed to the canopy skirt hem, and the component of the canopy aerodynamic inflating force, F_{AC}, is in equilibrium with the collapsing component of the suspension line force, F_{RL}, at the particular intermediate suspension line angle, β.

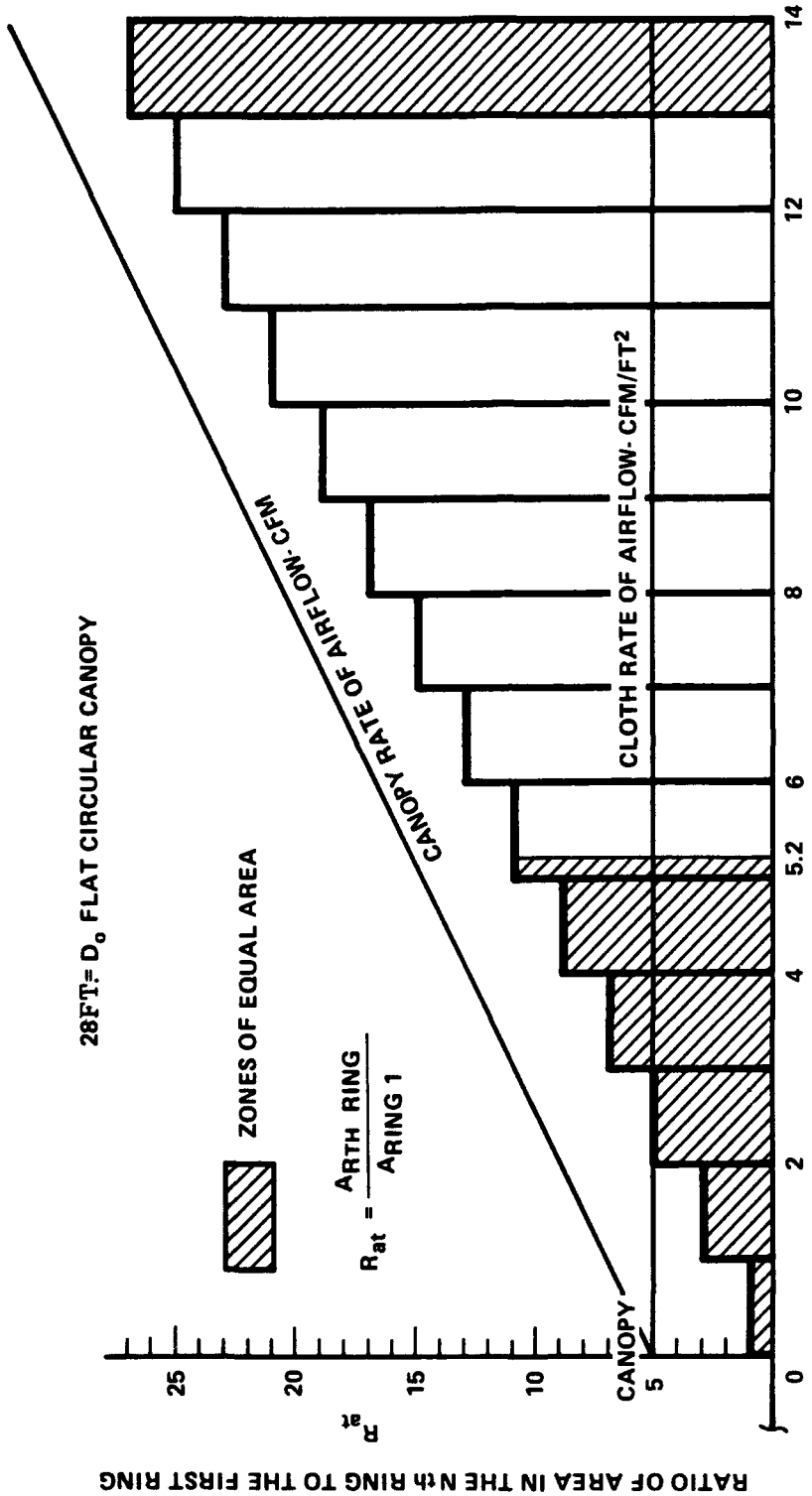

FIGURE 7. DISTRIBUTION OF CANOPY AREA AND RATE OF AIRFLOW VERSUS CANOPY RADIUS

A solution to critical inflation is to use more than one canopy cloth where the rates of flow per unit area decrease as the skirt hem is approached. This approach may also be applied to the porosity distribution of geometrically porous parachutes.

The inflation stability of a given parachute with a constant rate of canopy airflow per unit area depends upon the canopy diameter. As the diameter of the canopy ($D_o=2R_o$) increases by dR_o the surface area and canopy mouth area each increase.

$$A_{SO} = \pi R_o^2$$

$$A_{MO} = \pi R_{mo}^2$$

From Table 1 for a 30-gore flat circular parachute.

$$\frac{2\bar{a}}{D_o}=0.668;\frac{N}{\bar{a}}=0.827;\frac{b}{\bar{a}}=0.6214;\frac{b'}{\bar{a}}=0.7806$$

With reference to Figure 8.

$$\frac{d_{mo}}{2\bar{a}}=\frac{R_{mo}}{\bar{a}}\sqrt{1-\left(\frac{N/\bar{a}-b/\bar{a}}{b'/\bar{a}}\right)^2}$$

$$\frac{R_{mo}}{\bar{a}}=\sqrt{1-\left(\frac{0.827-0.6214}{0.7806}\right)^2}$$

$$\frac{R_{mo}}{\bar{a}}=0.965$$

$$\bar{a}=0.668\frac{D_o}{2}$$

$$R_{mo} = 0.965 \times 0.668 R_o$$

$$R_{mo} = 0.664 R_o$$

TABLE 1. SUMMARY OF 24- AND 30-GORE PARACHUTE TEST RESULTS

PARACHUTE TYPE		NO. OF GORES	SUSPENSION LINE LENGTH (ℓ_s) (IN)	VELOCITY		SCALE FACTOR, K2		N/$\bar{a}$	AXES RATIO			VOLUME IN^3			V_o/V_H
				MPH	FPS	$2\bar{a}/D_o$	$2\bar{a}/D_F$		$b/\bar{a}$	$b'/\bar{a}$	$b/\bar{a} + b'/\bar{a}$	V_H	V_c	V_o	
FLAT CIRCULAR*		24	34	50	73	.677	.679	.795	.5758	.8126	1.3884	4362	4695	7273	1.67
		30	34	17	25	.668	.669	.827	.6214	.7806	1.4020	4342	4626	7027	1.62
10% EXTENDED* SKIRT		24	34	100	147	.665	.648	.834	.5949	.8771	1.4720	4138	4446	6930	1.67
		30	34	17	25	.650	.633	.825	.6255	.7962	1.4127	4172	4076	6265	1.50
RING SLOT 16% GEOMETRICALLY POROUS		24	34	25	37	.663	.665	.824	.5800	.9053	1.4853	3591	3878	6031	1.68
		24	34	100	147	.680	.682	.819	.5800	.9053	1.4853	3591	4079	6510	1.81
		24	34	200	293	.694	.696	.809	.5800	.9053	1.4853	3591	4270	6924	1.93
		30	34	25	37	.677	.678	.788	.5800	.9053	1.4853	3582	3826	6404	1.79
		30	34	100	147	.684	.685	.802	.5800	.9053	1.4853	3582	4023	6588	1.84
		30	34	200	293	.698	.699	.800	.5800	.9053	1.4853	3582	4260	7012	1.96
RIBBON 24% GEOMETRICALLY POROUS		24	34	25	37	.671	.673	.770	.5980	.8187	1.4167	3591	3591	5968	1.66
		24	34	100	147	.676	.678	.813	.5980	.8187	1.4167	3591	3927	6097	1.70
		24	34	200	293	.687	.689	.804	.5980	.8187	1.4167	3591	4061	6389	1.78
		30	34	25	27	.655	.657	.782	.6021	.8463	1.4484	3582	3396	5666	1.58
		30	34	100	147	.669	.670	.784	.6021	.8463	1.4484	3582	3622	6022	1.68
		30	34	200	293	.677	.679	.823	.6021	.8463	1.4484	3582	4002	6256	1.75

*SINCE THIS PARACHUTE WAS "BREATHING" DURING THE TEST, SEVERAL PHOTOGRAPHS WERE TAKEN AT EACH SPEED. THE DATA WAS REDUCED FROM THE PHOTOGRAPH WHICH MOST REASONABLY APPEARED TO REPRESENT THE EQUILIBRIUM STATE.

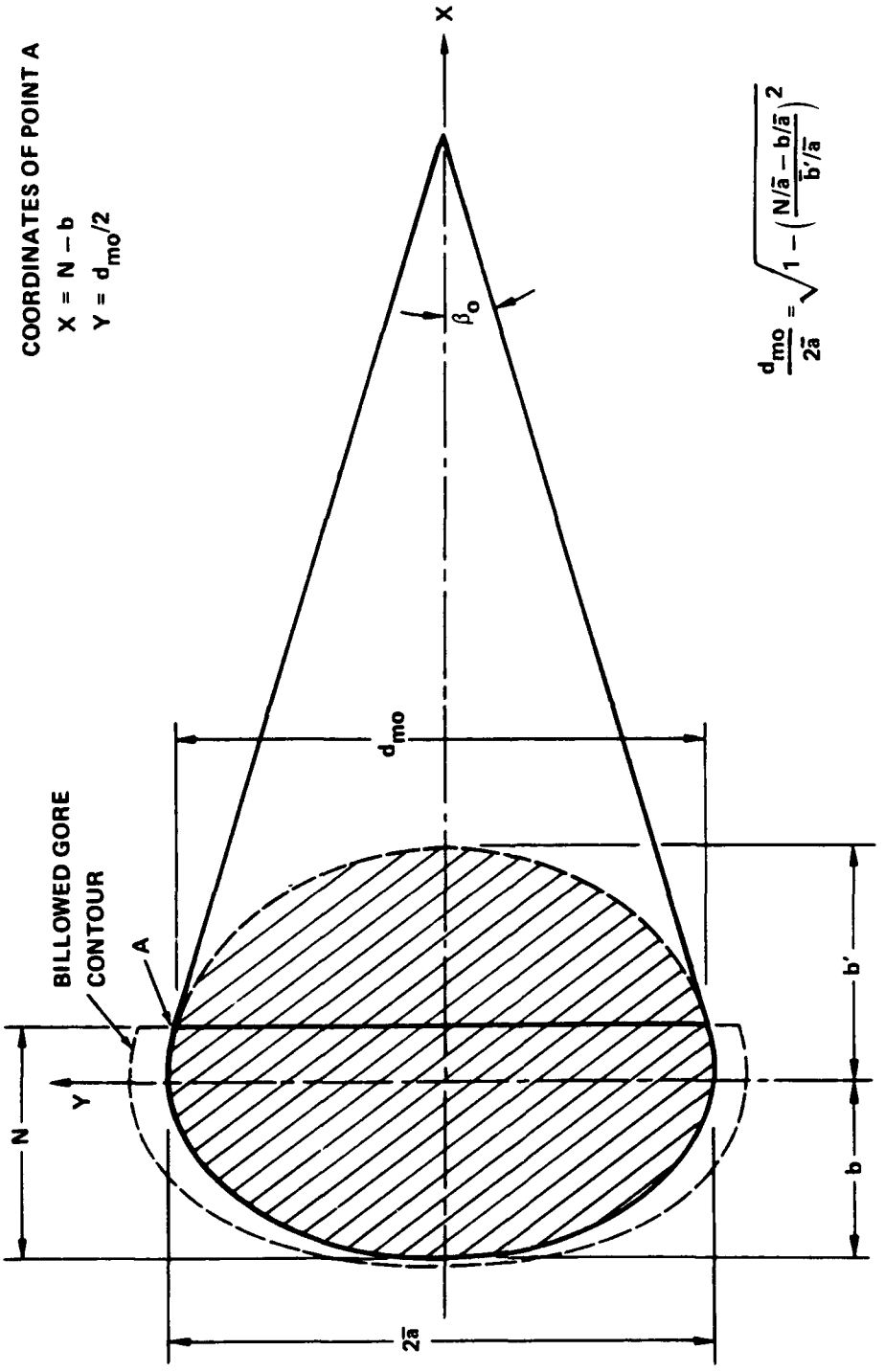

FIGURE 8. PARACHUTE CROSS SECTION NOMENCLATURE

The ratio of surface area to mouth area is:

$$\frac{A_{SO}}{A_{MO}} = \frac{\pi R_o^2}{\pi(0.644R_o)^2}$$

$$\frac{A_{SO}}{A_{MO}} = 2.41$$

and the ratio of mouth area to surface area is:

$$\frac{A_{MO}}{A_{SO}} = 0.415$$

If the inflated shapes of parachutes of similar proportions (D_o/L_e, number of gores, type) are taken to be essentially constant with size, the rate of increase in the A_{SO}/A_{MO} ratio must be the same for an increase in canopy diameter of dR_o.

Rate of change of surface area:

$$dA_{SO} = 2\pi R_o dR_o$$

Rate of change of mouth area:

$$dA_{MO} = 2\pi R_{mo}\, dR_{mo}$$

$$R_{mo} = 0.644R_o$$

$$dR_{mo} = 0.644\, dR_o$$

Rate of change of surface area to mouth area ratio

$$\frac{dA_{SO}}{dA_{MO}} = \frac{2\pi R_o dR_o}{2\pi(0.644R_o)(0.664dR_o)}$$

$$\frac{dA_{SO}}{dA_{MO}} = \frac{1}{0.664^2}$$

$$\frac{dA_{SO}}{dA_{MO}} = \frac{2.41}{1}$$

The implication of this is that as the parachute diameter is made larger, there are 2.41 FT^2 of outflow area generated at the flow sensitive canopy hem for each 1 FT^2 of inflow area generated. For a given rate of canopy airflow, there is a limit to the diameter of the parachute to maintain inflation stability. The A_{SO}/A_{MO} value may vary for different types of parachutes.

EFFECTIVE MOUTH AREA

Equation (1), Reference 2, expresses the inflation distance for solid cloth parachutes in terms of altitude and the system steady-state parameters imposed by the initial system design requirements.

$$V_s t_o = \frac{14W}{\rho g C_D S_o}\left[e^{\frac{\rho g \underline{V}_o}{2W}\left[\frac{C_D S_o}{A_{MO} - A_{SO}k\left(C_p\rho/2\right)^{1/2}}\right]} - 1\right] \tag{1}$$

The significance of the various terms is discussed in Reference 2. The most important term relevant to critical velocity is the concept of "effective mouth area," (A_{ME}).

$$A_{ME} = A_{MO} - A_{SO}k\left(C_p\rho/2\right)^{1/2}$$

As the rate of airflow per unit area determined by k, the air density, the pressure coefficient and the exponent 1/2 is increased the system has an effectively smaller inflow area. Since this affects the inflation reference time and distance exponentially, it is not necessary for the effective mouth area to reach zero before the parachute will fail to fully inflate. The exponential effect can extend the parachute inflation reference time and distance to a point where the canopy does not fully inflate during the system flight time. An observer on the ground would see an incomplete inflation. Equation (2) has the effective mouth area effect for a general value of "n".

$$\int_o^{\underline{V}_o} d\underline{V} = A_{MO}V_S \int_o^{t_o} \frac{\left(\frac{t}{t_o}\right)^6}{1+\frac{1}{7M}\left(\frac{t}{t_o}\right)^7} dt - A_{SO}k\left(\frac{C_p\rho}{2}\right)^n \int_o^{t_o}\left(\frac{t}{t_o}\right)^6\left[\frac{V_S}{1+\frac{1}{7M}\left(\frac{t}{t_o}\right)^7}\right]^{2n} dt \tag{2}$$

DETERMINATION OF CRITICAL VELOCITY

The basic parachute inflation mass flow equation is:

$$\dot{m}_P = \rho \frac{dV}{dt} = m \text{ inflow} - m \text{ outflow}$$

$$\dot{m}_P = \rho \frac{dV}{dt} = \rho V A_M - \rho P A_S$$

If at any time during the inflation process, the inflow is equal to the outflow the inflation process ceases.

$$\dot{m}_P = \rho V A_M - \rho P A_S = 0 \tag{3}$$

$$\frac{A_M}{A_S} = \frac{\rho P}{\rho V} = \frac{P}{V} = M'$$

where M' was shown in Reference 2 to be

$$M' = \frac{k\left(C_p \rho V^2 / 2\right)^n}{V} \tag{4}$$

When the ratio of the instantaneous mouth area, A_M, to the instantaneous inflated surface area, A_S, is equal to the mass flow rate ratio a critical inflation condition exists and $V=V_{cr}$.

$$\frac{A_M}{A_S} = \frac{k\left(C_p \rho V_{cr}^2 / 2\right)^n}{V_{cr}} \tag{5}$$

$$\frac{A_M}{A_S} = k\left(\frac{C_p \rho}{2}\right)^n V_{cr}^{2n-1}$$

When n=0.5, M' is independent of velocity

$$V_{cr} = \left(\frac{A_M}{A_s k\left(C_p \rho / 2\right)^n}\right)^{\frac{1}{2n-1}} \tag{6}$$

The critical velocity of imporous parachutes (k=o) is infinite and the canopy always inflates. However, the exponent "n" is a second cloth flow parameter that affects critical velocity. Measured values of "n" range between 0.53 and 0.771. For a value of 1/2 the exponent in Equation (6) becomes infinite. So there are really two cloth airflow properties that affect the critical velocity of parachutes. It should be noted that if a value of "n" less than 0.5 exists, the exponent of Equation (6) becomes negative. This has the effect of inverting Equation (6) and producing effects which are contrary to observed effects such as imporous parachutes never inflate.

Equation (4) illustrates how the exponent "n," the constant "k," the test velocity and the air density all contribute to the cloth permeability and the mass flow rate per unit area ratio.

When the test velocity is multiplied by a factor of two, the rate of canopy inflow is doubled. The rate of canopy outflow would be raised to the fourth power if it were not regulated by "n." Table 2 illustrates the contribution to outflow regulation by the cloth characteristic "n"as velocity is increased.

An examination of Table 2 discloses the following:

1. When n=0.5, the ratio of outflow to inflow per unit area is not affected by velocity. The outflow to inflow ratio per unit area is constant.

2. As n approaches unity, the rate of outflow per unit area exceeds the rate of inflow per unit area.

3. As n approaches unity, the rate of canopy outflow per unit area accelerates.

4. As velocity increases, the effects noted in 2 and 3 are amplified.

For cloths having an n value exceeding 0.5 the rate of canopy outflow per unit area accelerates as n approaches 1, and also as the velocity increases. Because of this, each parachute has some "CRITICAL VELOCITY" where the outflow is equal to the inflow. The designer must guarantee that the critical velocity of the design is safely above the range of operational velocities in order to produce a reliable design.

The increase in flow rate per unit area with velocity for values of n>0.5 explains why a fully inflated parachute will collapse when the critical velocity is reached. As the test velocity is raised, the following continuously varying events are in progress.

TABLE 2. EFFECTS OF THE EXPONENT "n" AND VELOCITY VARIATION ON THE CLOTH RATE OF AIRFLOW

	VELOCITY							
	2V		3V		4V			
n	2^{2n}	$\frac{O.F.^*}{I.F.}$	3^{2n}	$\frac{O.F.}{I.F.}$	4^{2n}	$\frac{O.F.}{I.F.}$	kt	CLOTH
0.5	2.00	1.00	3.00	1.00	4.00	1.00		
0.5260	2.07	1.04	3.18	1.06	4.30	1.07	2.757	MIL-C-17208, TYPE I, CLASS B
0.55	2.14	1.07	3.35	1.12	4.59	1.15		
0.5740	2.22	1.11	3.53	1.18	4.91	1.23	0.9947	MIL-C-8021, TYPE I
0.6	2.30	1.15	3.74	1.25	5.28	1.32		
0.6049	2.31	1.16	3.78	1.26	5.35	1.34	0.4412	MIL-C-8021 TYPE II
0.6126	2.34	1.17	3.84	1.28	5.47	1.37	7.43	3 MOMME SILK
0.6325	2.40	1.20	4.01	1.34	5.78	1.45	1.46	MIL-C-7020, TYPE III
0.65	2.46	1.23	4.17	1.39	6.06	1.52		
0.7	2.64	1.32	4.66	1.55	6.96	1.74		
0.75	2.83	1.41	5.20	1.73	8.00	2.00		
0.7716	2.91	1.46	5.45	1.82	8.49	2.12	0.0415	MIL-C-7219, TYPE II
0.8	3.03	1.52	5.80	1.93	9.19	2.30		
0.85	3.25	1.63	6.47	2.16	10.56	2.64		
0.9	3.48	1.74	7.22	2.41	12.13	3.03		
0.95	3.73	1.87	8.06	2.69	13.93	3.48		
1.00	4.00	2.00	9.00	3.00	16.00	4.00		

* O.F. = outflow; I.F. = inflow ; EQ (VI-26a)

† k is in cubic feet per square foot per second

1. The ratio of the rate of outflow per unit area to the rate of inflow per unit area, M', is rising.

2. The higher rate of outflow coupled with the concentrated outflow area at the hem, as in Figure 7, increases the canopy outflow volume per unit of time.

3. The higher outflow volume reduces the canopy internal pressure which also reduces the pressure differential across the canopy cloth.

4. The reduced canopy cloth pressure differential lowers the canopy inflation force, F_{AC}, at the canopy hem.

5. The parachute drag force has been rising which causes the canopy collapsing component of the suspension line force, F_{RL}, at the hem to increase.

6. At the critical velocity the inflation force, F_{AC}, becomes less than the collapsing force, F_{RL}, and the canopy outflow volume also exceeds the inflow volume. Both of these conditions contribute to canopy collapse.

7. The canopy continues to collapse until the higher flow rate per unit area passing through the reduced canopy inflated area can produce a new canopy inflating aerodynamic force, F_{AC}, which is in equilibrium with the new collapsing force component, F_{RL}, of the reduced suspension line force at a pseudo hem where the inflated and uninflated canopy areas meet. The suspension line force has been reduced do to the smaller canopy inflated diameter and the canopy collapsing component is further reduced by a smaller suspension line angle, β .

Fully inflated parachutes possess a zone ahead of the skirt hem where the local static pressure is higher than free stream static pressure. This static pressure zone decays as the distance ahead of the canopy skirt hem increases. Figure 9 presents a static pressure profile measured along the centerline of a Cross-type parachute during a subsonic wind tunnel test. Figure 9A is a photograph of the Cross parachute under test. Figure 10 presents the effects of canopy cloths with different rates of airflow on the drag coefficients of geometrically similar 41 percent scale models of the U.S. Navy MK 38 MOD 0 Cross parachute. The 3-momme silk cloth canopy partially inflated to the point where the lowered canopy pressure differential, due to the rate of airflow, acting on the canopy surface area balanced the radial component, F_{RL}, of the suspension line force.

The flow rate contribution of the air density of Equation (4) is also regulated by the exponent "n". Table 3 illustrates the reduction in cloth flow rate as "n" approaches one for selected altitudes from sea level to 100,000 feet.

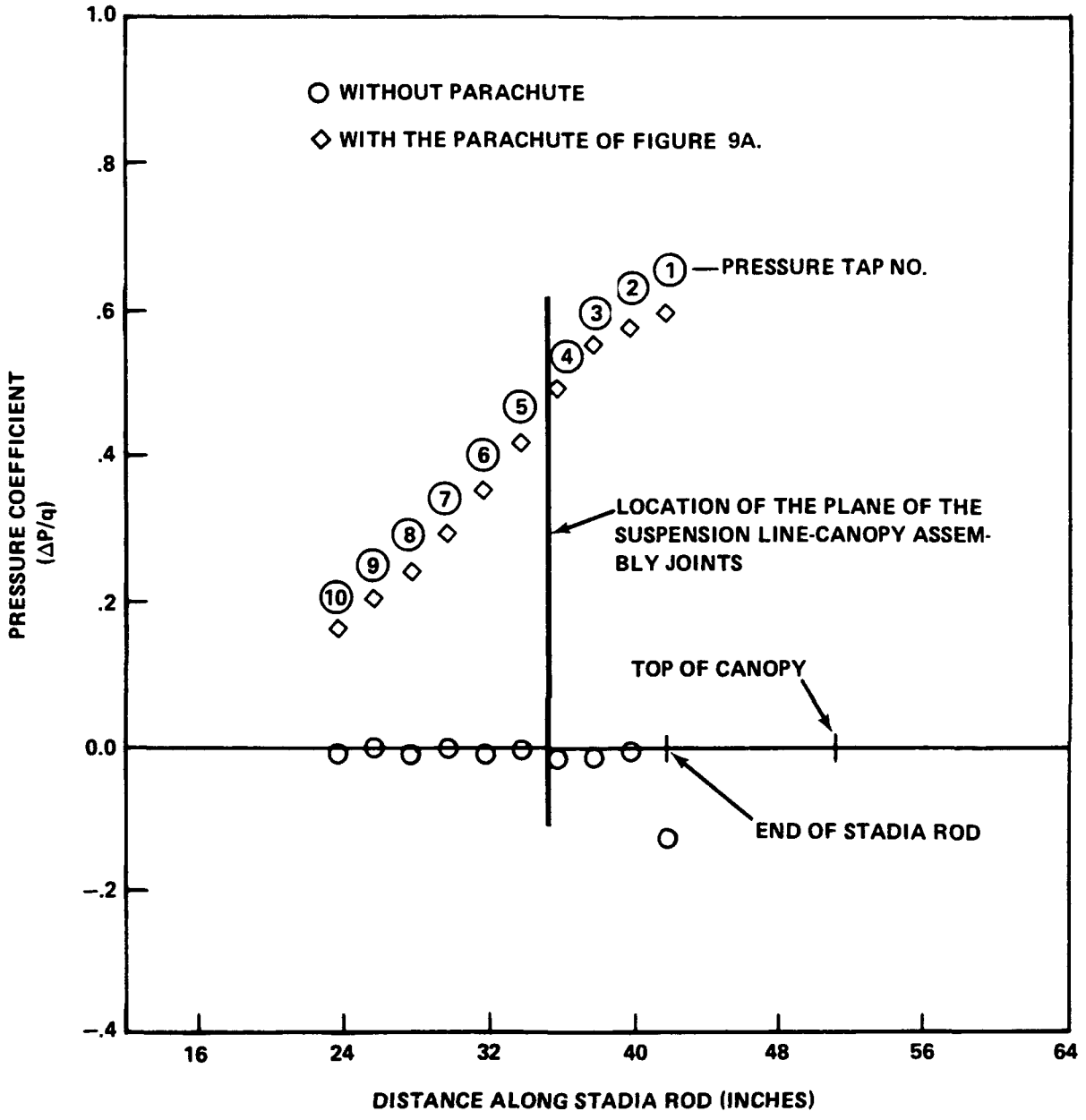

TEST VELOCITY 200 MPH

FIGURE 9. MEASURED STATIC PRESSURE DISTRIBUTION ALONG THE STADIA ROD SHOWING ELEVATED LOCAL STATIC PRESSURES AHEAD OF THE CANOPY SKIRT HEM.

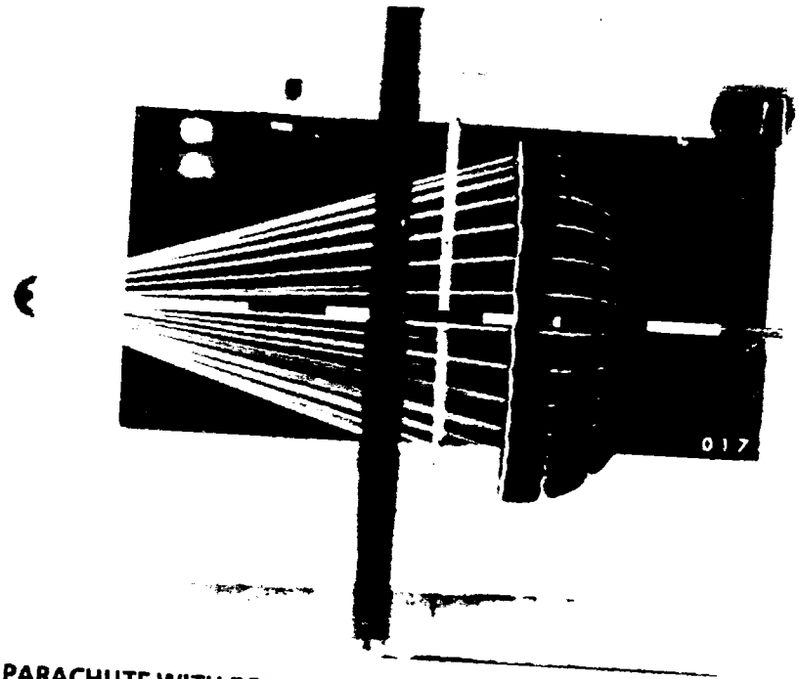

RINGSLOT PARACHUTE WITH EQUALLY ELONGATED SUSPENSION LINES AT 200 MPH

D_0 = 37½ INCH DIA
24 GORE
16% POROSITY

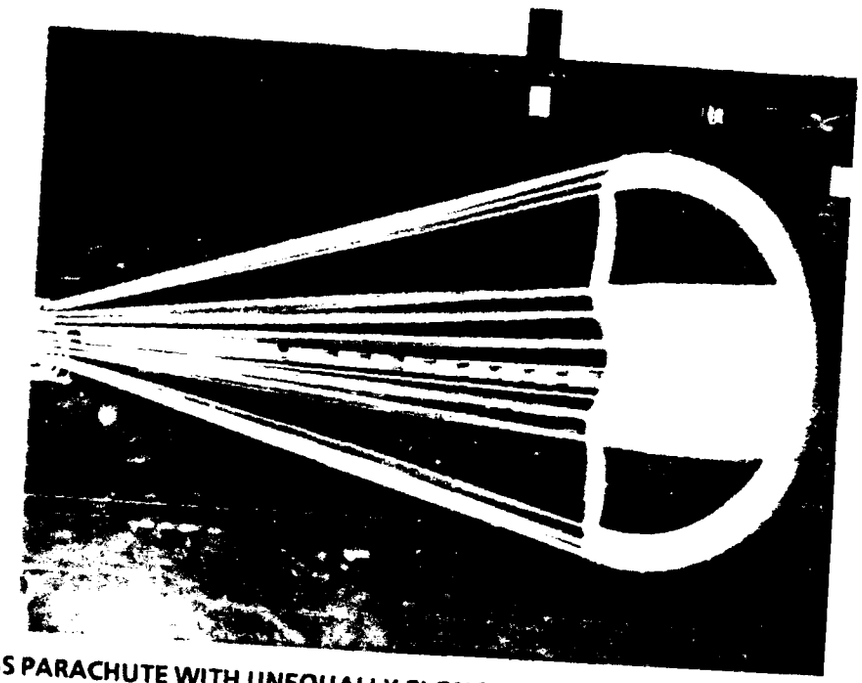

CROSS PARACHUTE WITH UNEQUALLY ELONGATED SUSPENSION LINES AT 200 MPH

L = 40 INCH DIA
W/L = 0.264

FIGURE 9A. PHOTOGRAPH OF THE CROSS PARACHUTE OF FIGURE 9 IN THE WIND TUNNEL

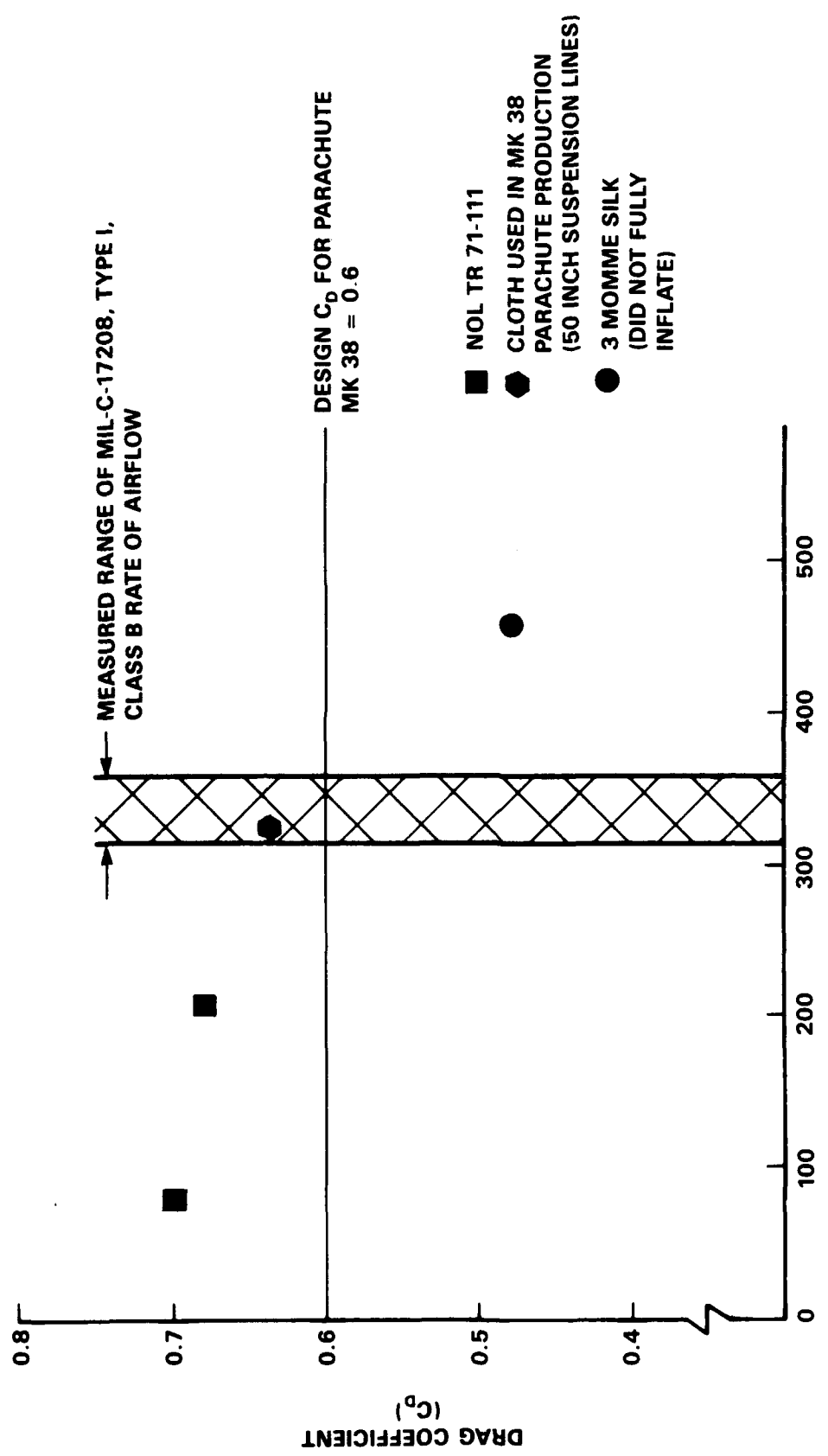

FIGURE 10. EFFECT ON THE CLOTH RATE OF AIRFLOW ON THE DRAG COEFFICIENT OF THE MK 38 MOD 0 PARACHUTE.

TABLE 3. EFFECTS OF THE EXPONENT "n" AND DENSITY RATIO ON THE CLOTH RATE OF AIRFLOW

	DENSITY FACTOR $(\rho/\rho_o)^n$						
ALTITUDE (FT.)	SEA LEVEL	20k	40k	60k	80k	100k	
n \ ρ/ρ_o	1.000	0.5332	0.2471	0.09491	0.03606	0.01396	CLOTH
0.5	1.000	0.7302	0.4971	0.3081	0.1899	0.1182	
0.5260	1.000	0.7184	0.4793	0.2898	0.1742	0.1057	MIL-C-17208, TYPE I, CLASS B
0.55	1.000	0.7076	0.4635	0.2739	0.1608	0.0954	
0.5740	1.000	0.6970	0.4482	0.2588	0.1485	0.0861	MIL-C-8021, TYPE I
0.6	1.000	0.6857	0.4322	0.2434	0.1362	0.0771	
0.6049	1.000	0.6836	0.4293	0.2406	0.1340	0.0755	MIL-C-8021, TYPEII
0.6126	1.000	0.6803	0.4247	0.2363	0.1306	0.0730	3 MOMME SILK
0.6325	1.000	0.6718	0.4130	0.2255	0.1223	0.0671	MIL-C-7020, TYPE III
0.65	1.000	0.6645	0.4030	0.2164	0.1154	0.0622	
0.7	1.000	0.6439	0.3758	0.1924	0.0977	0.0503	
0.75	1.000	0.6240	0.3505	0.1710	0.0828	0.0406	
0.7716	1.000	0.6156	0.3400	0.1625	0.0770	0.0307	MIL-C-7219, TYPE III
0.8	1.000	0.6047	0.3268	0.1520	0.0701	0.0328	
0.85	1.000	0.5859	0.3047	0.1351	0.0594	0.0265	
0.9	1.000	0.5678	0.2842	0.1201	0.0503	0.0214	
0.95	1.000	0.5502	0.2650	0.1068	0.0426	0.0173	
1.00	1.000	0.5332	0.2471	0.09491	0.0361	0.0140	

EFFECT OF ALTITUDE ON PARACHUTE INFLATION TIME, STABILITY AND DRAG COEFFICIENT

The mass flow rate ratio, M', provides explanations as to why solid cloth parachutes inflate faster as the deployment altitude is raised, otherwise stable parachutes are caused to oscillate and also the shape of the basic dynamic drag area inflation signature.

It is well known from field tests that solid cloth parachutes inflate faster as the altitude rises and the air becomes less dense. This apparent paradox can be explained by the examination of the mass flow ratio. The explanation is simplified by using an infinite mass deployment to eliminate transient velocity profiles that vary with altitude during inflation.

If a given solid cloth parachute system were tested under infinite mass conditions in a variable density wind tunnel, the canopy inflates in a predictable time at sea level density. The mass flow ratio is in accordance with Equation (4a) and

$$M' = \frac{k\left(C_{pav}\rho_o V^2/2\right)^n (\rho/\rho_o)^n}{V} \qquad (4a)$$

$\rho/\rho_o = 1$. When the wind tunnel density is reduced to $\rho/\rho_o = 0.5$ (approximately 22,000 feet) and the parachute retested at constant velocity, the mouth inflow rate per unit area and the velocity contribution to the canopy outflow rate per unit area is the same as at sea level deployment. However, the cloth pressure differential is reduced due to the lower air density which results in a reduced rate of canopy outflow as illustrated in Figure (11). Under a condition of constant canopy mouth inflow rate and reduced canopy outflow rate the parachute must inflate more rapidly.

In a constant dynamic pressure scenario test condition the cloth rate of airflow per unit area remains the same at all altitudes, but to achieve constant dynamic pressure the test velocity must be raised. So under constant dynamic pressure conditions, the canopy rate of outflow per unit area is the same at all altitudes and the rate of mouth inflow per unit area increases, which once again results in a reduced inflation time.

Some analysts suggest that the canopy cloth is less porous as the altitude is increased. It appears that the rate of airflow of the canopy cloth is the same at all altitudes for a given ΔP and the change in performance is due to the pressure differential variations altering the cloth rate of airflow per unit area. A reduction in pressure differential and cloth rate of airflow (inflation time reduction, opening shock increased, larger canopy oscillations) may give the parachute system the attributes of a lower permeability cloth near sea level.

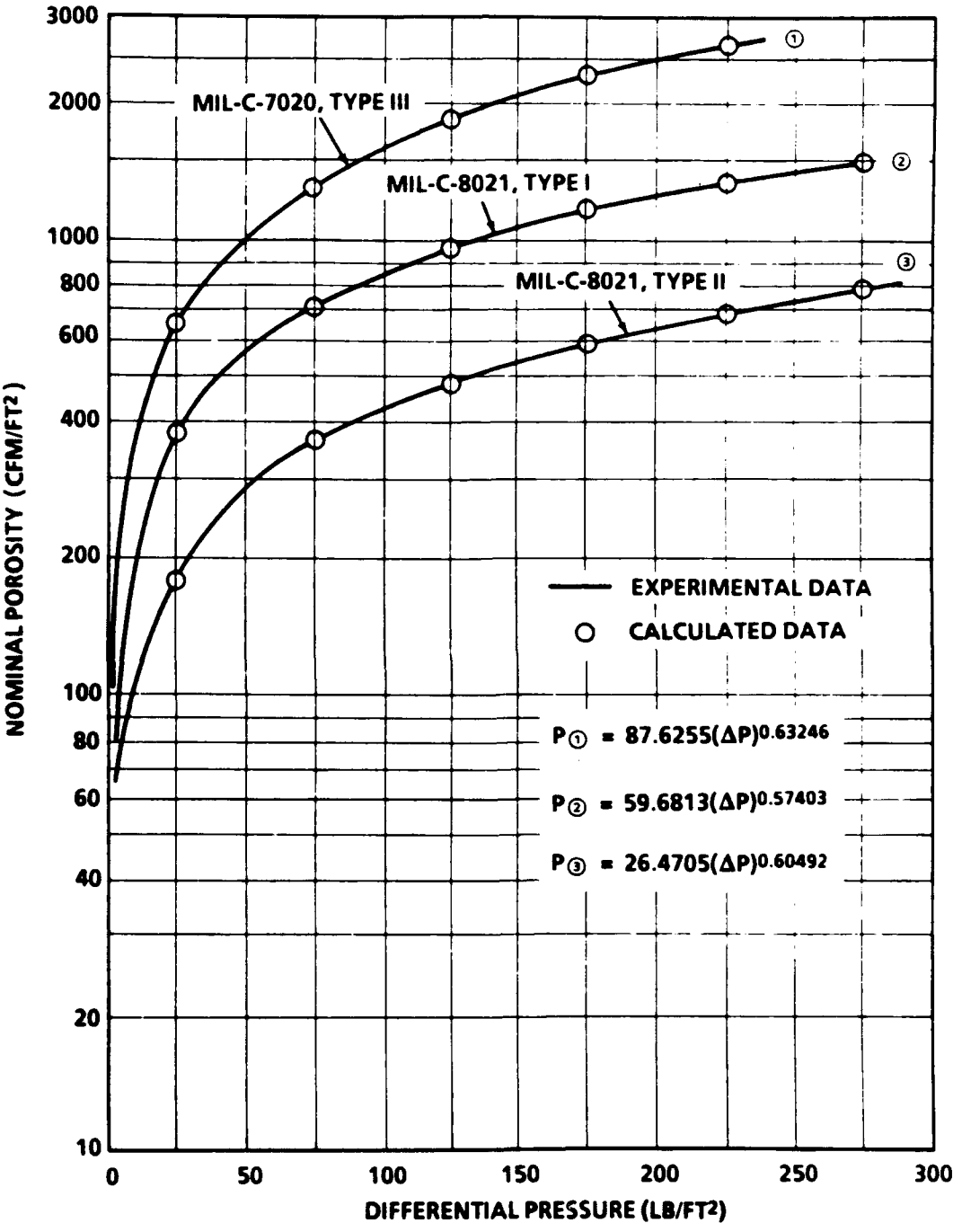

FIGURE 11. NOMINAL POROSITY OF PARACHUTE MATERIAL VERSUS DIFFERENTIAL PRESSURE

During low altitude finite mass deployments the inflating parachute system has substantial velocity reduction while in the inflation process. The inflation velocity profile at say 22,000 FT is greater than the sea level inflation velocity profile for constant velocity or constant dynamic pressure deployment scenarios do to the decrease in the air density. Equations (1), (7), and (8) were developed in Reference 2. Equation (1) shows that the inflation distance of a solid cloth parachute depends upon the deployment altitude, cloth rate of airflow, system mass, and the parachute steady-state geometry.

$$V_s t_o = \frac{14W}{\rho g C_D S_o}\left[e^{\frac{\rho g y_o}{2W}\left[\frac{C_D S_o}{A_{MO} - A_{SO} k (C_p \rho / 2)^{1/2}}\right]_{-1}} \right] \tag{1}$$

The inflation distance and altitude determine the Ballistic Mass Ratio scale parameter, M.

$$M = \frac{2W}{\rho g V_s t_o C_D S_o} \tag{7}$$

and the Ballistic Mass Ratio determines the velocity profile during inflation.

$$\frac{V}{V_S} = \frac{1}{1 + \frac{1}{7M}\left(\frac{t}{t_o}\right)^7} \tag{8}$$

All of these effects result in faster opening of the parachute. So the apparent paradox of the decrease in solid cloth parachute inflation time as the air density is reduced is not a paradox at all. It is as it should be! The reduction of cloth outflow versus altitude is shown in Figures (12) and (13).

Parachutes with low values of canopy cloth permeability are known to oscillate. As the canopy cloth permeability is raised, the oscillations decrease. Cross parachutes with a W/L of 0.264 oscillate violently in wind tunnels when the cloth permeability is 8 CFM/FT^2 at 1/2 inch of water pressure. The same canopy geometry with MIL-C-7020 canopy cloth has minimal oscillations in the wind tunnel. Cross parachutes with a W/L of 0.264, MIL-C-7020 canopy cloth, and "L" diameters in the range 60 to 75 feet oscillate noticeably when deployed above 200,000 feet.

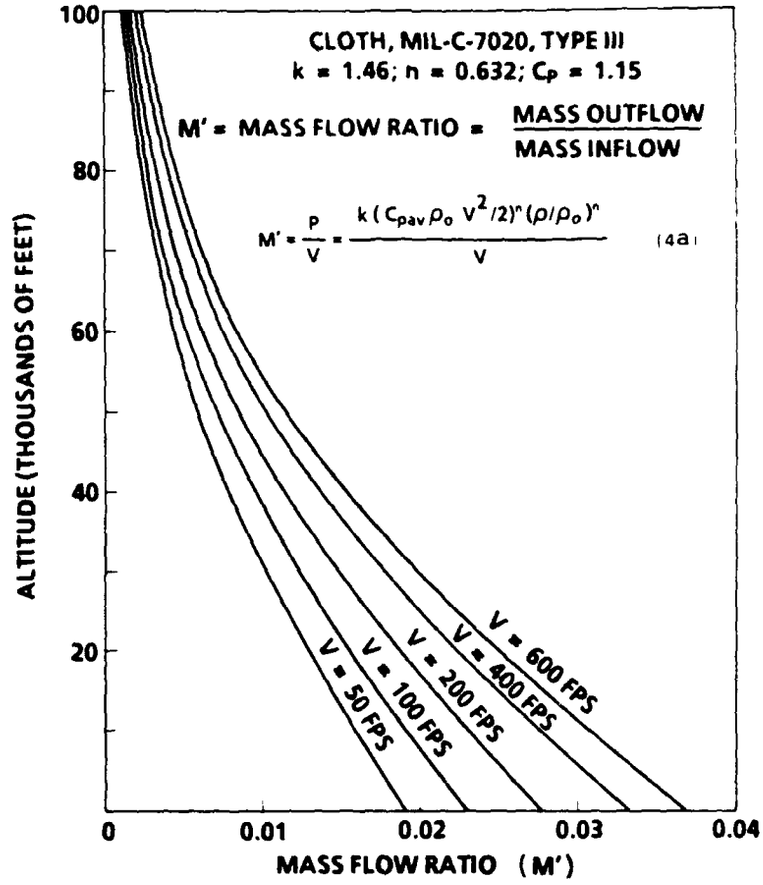

FIGURE 12. EFFECT OF ALTITUDE ON MASS FLOW RATIO AT CONSTANT VELOCITY

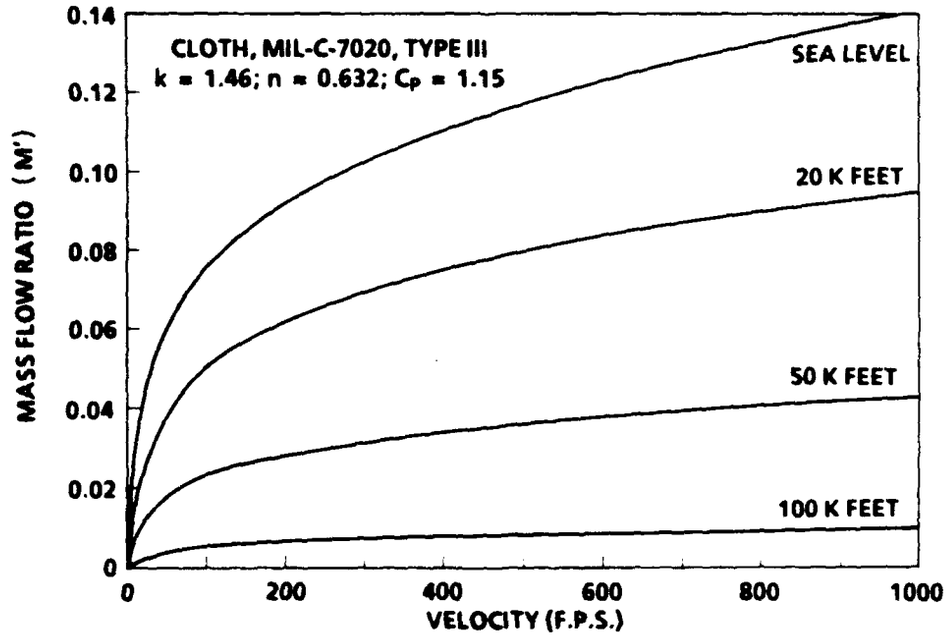

FIGURE 13. EFFECT OF VELOCITY ON MASS FLOW RATIO AT CONSTANT DENSITY

At these altitudes the low air density has degraded the flow rate through the canopy cloth and just as the wind tunnel tests demonstrated low cloth rate of airflow correlates with more oscillation.

Figure 10 Cross parachute drag coefficient versus canopy cloth rate of airflow shows a decrease in drag coefficient as canopy permeability increases. The permeabilities noted are the values measured at 1/2 inch of water pressure. Some of the implications of the drag coefficient data are:

a. At a constant altitude there may be a decrease in drag coefficient with increased test velocity. Depending on the cloth, the effect may be negligible.

b. As the test altitude rises, in a constant velocity scenario, the cloth permeability decreases do to reduced density and drag coefficients tend to be increased.

EFFECT OF MASS FLOW RATIO ON THE PARACHUTE DYNAMIC DRAG AREA SIGNATURE

The recorded infinite mass inflation signatures of solid cloth parachutes show that the inflation process begins slowly until the canopy reaches an inflation time ratio of approximately $t/t_o=1/2$. As inflation continues the rate of inflation increases with time. The mass flow rate ratio, M', is also part of the mechanics of the inflation process. Equation (9) and Table 2 have demonstrated how the ratio of the rate of outflow per unit area to rate of inflow per unit area increases as the velocity is raised. An inflating parachute is slowing down the payload with the following continuously varying sequence of events:

1. In the initial phase of inflation the canopy inlet area is small and the volume of air collected is small.

2. Due to the small parachute drag area the inflation process, up to approximately $t/t_o=1/2$ is essentially at constant velocity and M' is essentially constant.

3. After $t/t_o=1/2$, the canopy begins to develop a drag area that is effective in reducing the trajectory velocity.

4. Just as increasing the wind tunnel test velocity raised the cloth outflow per unit area to inflow per unit area ratio, the reduction of trajectory velocity lowers the ratio of outflow per unit area to inflow per unit area and the canopy retains more of the inflow volume.

5. As the canopy retains more of the inflow volume the rate of inflation increases and the larger parachute further retards the payload.

6. A continuous inflation cycle of slow down reduces the rate of outflow per unit area, retains more of the inflow through the increasing mouth area, and increases the rate of inflation. Slow down has been generated that seems to explain the deployment signature of solid cloth parachutes. For finite mass and infinite mass drag area-deployment time signatures to be the same, this effect must be small compared to the inflation process dynamics. In Table 1 of Reference 3 the unfolding phase of inflation velocity profile is given by Equation (8) for $\tau=0$ and j=6.

$$\frac{V}{V_S}=\frac{1}{1+\frac{1}{7M}\left(\frac{t}{t_o}\right)^7} \tag{8}$$

Substitution of the velocity expression into the mass flow rate ratio Equation (9)

$$\frac{P}{V}=k\left(C_{pav}\rho/2\right)^n V^{2n-1} \tag{9}$$

yields

$$\frac{P}{V}=\frac{k\left(C_{pav}\rho/2\right)^n V_S^{2n-1}}{\left[1+\frac{1}{7M}\left(\frac{t}{t_o}\right)^7\right]^{2n-1}} \tag{10}$$

$$\frac{P}{V}=\left(\frac{P}{V_S}\right)\frac{1}{\left[1+\frac{1}{7M}\left(\frac{t}{t_o}\right)^7\right]^{2n-1}} \tag{10a}$$

The particular mass flow rate ratio is the infinite mass flow rate ratio divided by a reduction factor represented by the denominator of Equation (10a) which depends upon the mode of operation, infinite mass, intermediate mass, or finite mass. The percent reduction in the mass flow rate ratio is given by the difference between the infinite mass operation and the particular operational ballistic mass ratio.

$$\left(\frac{P}{V}\right)_{Reduction}=\left(\frac{P}{V_s}\right)\left(1-\frac{P}{V}\right)x100 \tag{11}$$

For infinite mass deployments, $M=\infty$, and the mass flow rate ratio is constant throughout the inflation. A value of M=10, for solid cloth parachutes, is a nearly constant velocity deployment. Table 4 summarizes the variation of the mass flow rate ratios for several ballistic mass ratio applications.

Table 4 shows that the reduction in the mass flow rate ratio is not significant except in the later stages of very finite mass deployments. Therefore, this condition does not significantly vary the drag area ratio-inflation time ratio signature.

EXAMPLE 1 A parachute is fully inflated in a wind tunnel. As the wind tunnel velocity is increased, the parachute suddenly collapses. Explain what has happened.

If the wind tunnel is maintained at the critical velocity, and the air density is reduced, what effects are expected?

When the parachute is fully inflated at a wind tunnel velocity below the critical velocity, explain the effects that are expected as the D_o diameter is allowed to increase?

Discussion: The events which occur during the collapse of a critical parachute are controlled by the generation and distribution of the parachute aerodynamic forces and canopy rate of airflow. Currently, four forces have been identified as contributing to the total critical condition. Three of these forces regulate the upper critical velocity of the canopy collapse. After collapse, an additional fourth force is generated which delays reinflation until the lower critical velocity is achieved. The four forces are:

1. Parachute drag force, F_D.

2. Radial component of the suspension line force, F_{RL}. This force, perpendicular to the parachute centerline at the canopy skirt hem-suspension line junction, is a result of the suspension line cone angle and tends to collapse the canopy.

3. Radial component of the canopy aerodynamic inflation force, F_{AC}. This force develops from the canopy pressure differential acting on the canopy cloth and tends to inflate the canopy. The pressure differential is dependent on the quantity of air permitted to pass through the canopy surface. For a given constant canopy cloth k and n, this varies with velocity and altitude.

TABLE 4. EFFECTS OF BALLISTIC MASS RATIO ON THE REDUCTION OF THE MASS FLOW RATE RATIO DURING THE UNFOLDING PHASE OF INFLATION OF A FLAT SOLID CLOTH PARACHUTE.

n = 0.632

BALLISTIC MASS RATIO	M = ∞		M = 10		M = 1		M* = 0.1		M* = 0.01	
MASS FLOW RATE RATIO / t/t_o	$\frac{P}{V}$	$1-\frac{P}{V}$ %	$\frac{P}{V}$	$1-\frac{P}{V}$ %	$\frac{P}{V}$	$1-\frac{P}{V}$ %	$\frac{P}{V}$	$1-\frac{P}{V}$ %	$\frac{P}{V}$	$1-\frac{P}{V}$ %
0	1.0	0.00	1.000	0.00	1.0	0.00	1.000	0.00	1.000	0.00
0.2	1.0	0.00	1.000	0.00	1.0	0.00	1.000	0.00	1.000	0.00
0.4	1.0	0.00	1.000	0.00	1.0	0.00	0.999	0.06	0.994	6.10
0.6	1.0	0.00	0.999	0.01	0.999	0.11	0.990	1.00	0.915	8.50
0.8	1.0	0.00	0.999	0.08	0.992	0.78	0.933	6.68	0.694	30.6
1.0	1.0	0.00	0.996	0.37	0.965	3.46	0.791	20.90	0.487	51.3

*LIMITING BMR FOR FINITE MASS OPERATION; $M_L = 0.1907$

4. Parachute squid force, F_{SQ}. After a critical canopy has collapsed, the collapsed shape deflects the airflow symmetrically around the canopy in a manner different from the fully inflated state. This additional symmetrical inward force tends to hold the canopy in the collapsed state and stabilizes the configuration.

a) Collapse at the critical velocity:

(1) When the critical parachute is already inflated below the critical velocity, the volume of flow into the canopy through the mouth is equal to the volume of outflow through the canopy surface. The canopy cloth pressure differential, at this velocity, provides an inflation force, F_{AC}, at the canopy hem that balances the collapsing radial component, F_{RL}, of the parachute suspension line force, Figure 4.

(2) As the wind tunnel velocity is increased the ratio of the rate of outflow through the cloth per unit area to the rate of inflow through the mouth per unit area, M', continuously increases (see Table 2) and the outflow through the canopy skirt area increases due to the distribution of the cloth area in the gore, Figure 7.

(3) The increased rate of canopy airflow causes a reduction in the canopy cloth pressure differential. This produces an effect similar to the geometrically porous canopies of Figure 14 where increasing canopy porosity for constant suspension line length results in a smaller inflated canopy diameter, caused by a lower internal pressure. If the canopy surface area is used in the data reduction the lower parachute aerodynamic drag force, due to the smaller inflated diameter, manifests itself as a reduction in the drag coefficient.

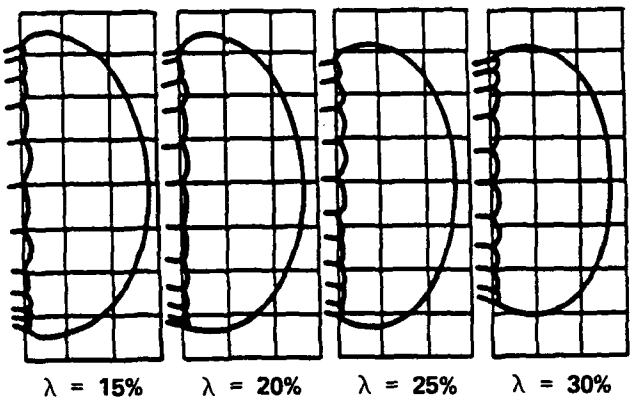

FIGURE 14. SIDE PROFILES OF RIBBON PARACHUTE CANOPIES WITH POROSITIES FROM 15 TO 30 PERCENT

Figure 15 illustrates the effect of canopy cloth rate of airflow on the pressure distribution measured adjacent to the centerline of the Cross parachute MK 38 MOD 0. All parachute models were of common geometry with varied canopy cloth permeabilities.

(4) As the critical velocity is approached, the ratio of the rate of canopy outflow per unit area to canopy inflow per unit area continuously increases. Also, the aerodynamic drag force and the radial component of the suspension line force increases. At the critical value, the inflating canopy pressure differential at the hem has been lowered to a point where the canopy aerodynamic force at the hem, F_{AC}, is insufficient to resist the suspension line collapsing force, F_{RL}, and the canopy collapses to a condition where the inflow through the smaller canopy mouth is equal to the outflow of the higher flow rate per unit area through the reduced inflated canopy area.

b) Density reduction: The air density affects the rate of canopy outflow per unit area in the mass flow rate ratio, M', the canopy drag force and F_{RL}. Density reduction results in a corresponding reduction of canopy outflow rate per unit area and tends to support canopy inflation, see Table 3. When the wind tunnel density is sufficiently reduced the ratio of canopy outflow rate to mouth inflow rate is less than one, and the canopy reinflates since F_{RL} has also been reduced.

	RUN NO.	PARACHUTE NO.	NO. LINES	CANOPY CLOTH	PERMEABILITY (CFM/FT^2)
×	5	2	16	MIL-C-7020, TYPE I	90
○	11	8	16	MIL-C-17208, TYPE I, CLASS B	325
◇	12	9	16	MIL-C-17208, TYPE I, CLASS B	325
△	13	10	16	3 MOMME SILK	428
○	14	STRUT AND FIXTURE TARE RUN WITH LONG STADIA ROD			

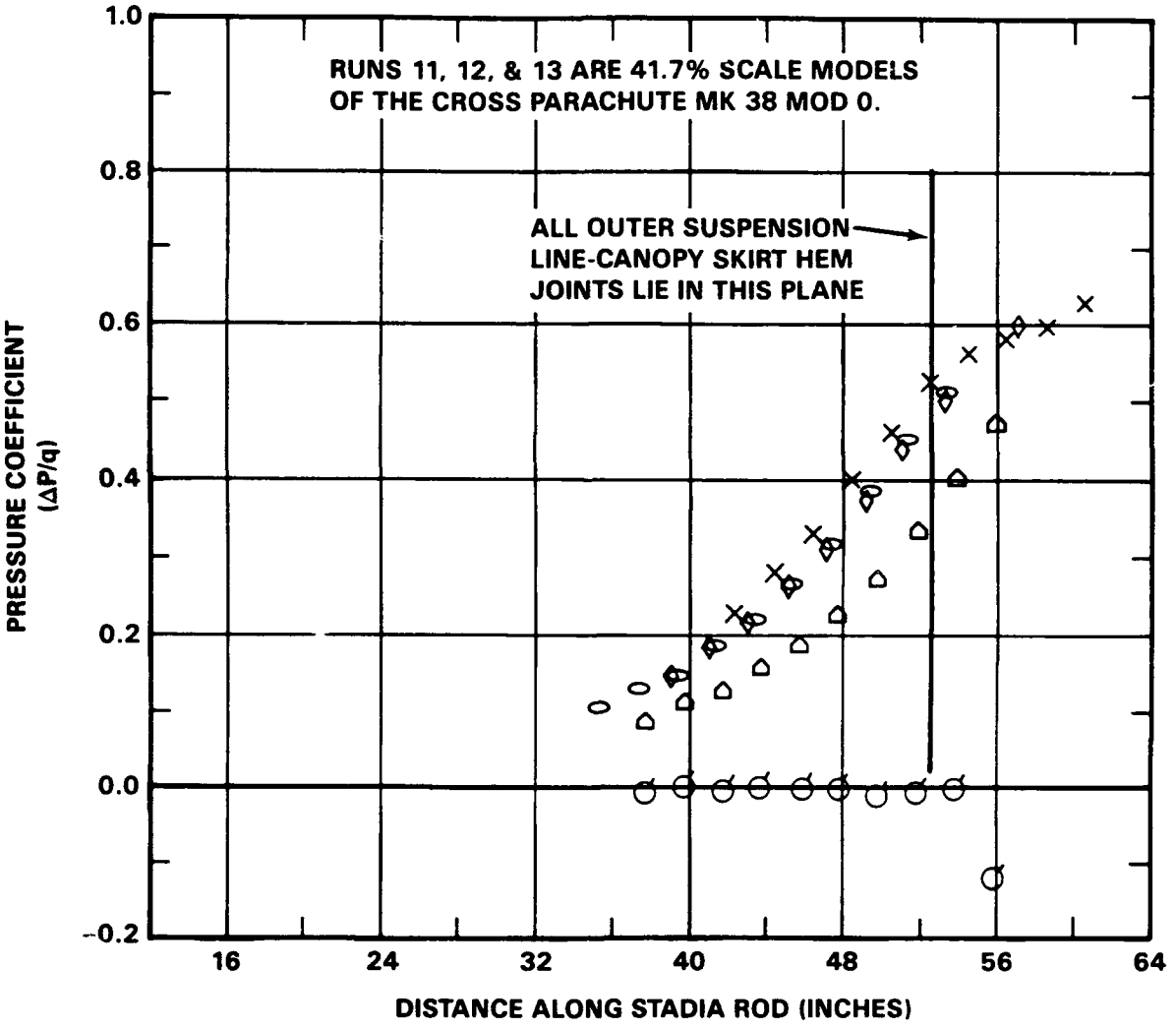

TEST VELOCITY 200 MPH

FIGURE 15. EFFECT OF CLOTH PERMEABILITY ON THE MEASURED STATIC PRESSURE DISTRIBUTION ALONG THE STADIA ROD SHOWING ELEVATED LOCAL STATIC PRESSURES AHEAD OF THE CANOPY SKIRT HEM.

c) The reinflation velocity of a critical parachute, at constant density, is less than the critical velocity at collapse. In the collapsed squid like shape the redirected flow has modified the canopy force distribution as shown in Figure 16. In uniform flow, the newly introduced "squid" force which rings the canopy like a wide belt and acts inward toward the canopy centerline, contributes to the stability of the squidded canopy. This also applies to inflating noncritical canopies. Upon reduction of the wind tunnel velocity, the ratio of canopy outflow to inflow begins to decrease, the canopy drag force and the opposing collapsing component, F_{RL}, of the suspension line force are also getting smaller. At the upper critical velocity the canopy rates of airflow are marginal for reinflation. The canopy is kept from fully inflating by the collapsing squid force, F_{SQ}. Further velocity reduction lowers the mass flow rate ratio, M', increases the canopy internal pressure and reduces the collapsing force, F_{RL}. At the lower critical velocity conditions have modified to the point where the internal pressure front can override the reduced collapsing force, F_{SQ}, and the canopy reinflates.

d) Increase of D_o diameter: In the case of the variation of the D_o diameter, it has been shown that the canopy outflow surface area increases by 2.41 square feet for each square foot of increase of mouth inflow area derived from an increase in D_o. The increased canopy surface area is added at the skirt hem where the outflow is a maximum. An increasing D_o eventually results in a critical velocity condition.

Wind tunnel tests are planned to investigate the effects of the ratio of steady-state mouth area to surface area (A_{MO}/A_{SO}) and cloth rate of airflow on parachute critical velocity. Test results are to be published in Reference 1.

The various standard cloths available for parachutes are based on use properties such as strength, weight per square yard, elongation and air permeability. Cloth, ordered from and conforming to a specification, has nominal limits on the requirements. The rate of airflow, due to the nature of cloth manufacture has the permeability usually specified in a range from a lower limit to an upper limit. The upper limit may exceed the lower limit by 50 to 80 percent. In addition, the rate of airflow may vary randomly between limits within a roll of cloth or between different rolls of cloth of the same lot. In addition, different weavers may use different constructions to obtain the requirements of the specification. This may vary the airflow performance. Identical parachutes constructed at the same time, may have some what different opening characteristics because of variations in the manufactured cloth air permeability.

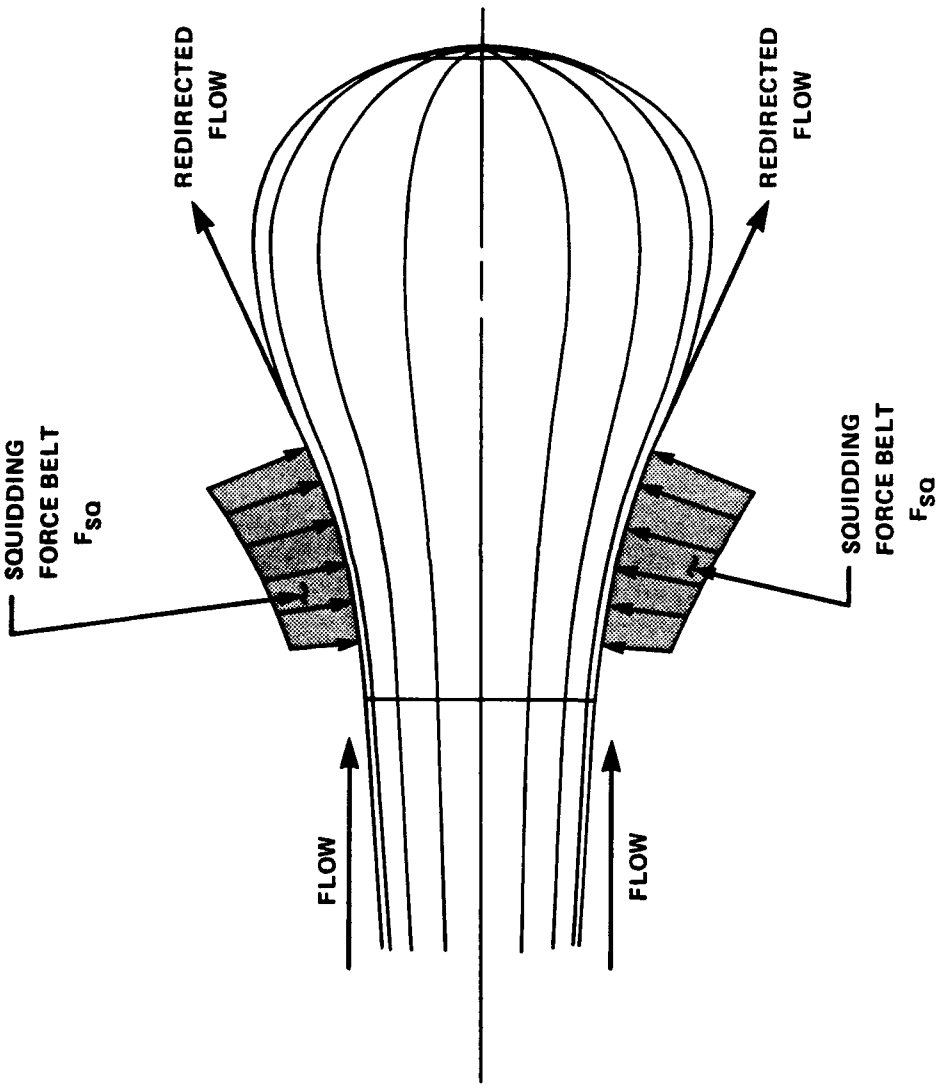

FIGURE 16. THE REDIRECTED FLOW AROUND A SQUIDDED OR INFLATING PARACHUTE DEVELOPS A SQUIDDING FORCE BELT WHICH STABILIZES THE ASSEMBLY AND MAINTAINS THE SQUIDDED CONDITION BELOW THE UPPER CRITICAL VELOCITY

CONCLUSIONS

1. Parachute inflation characteristics of solid flat types of canopies are determined by the balance between the radial canopy inflating aerodynamic force and the opposing deflating inward radial suspension line force component at the canopy skirt hem.

2. The parachute aerodynamic force may be increased by:

a. Reducing the canopy rate of airflow. This raises the canopy internal pressure which increases the canopy inflated diameter.

b. Using longer suspension lines, which permit greater inflation by reducing the collapsing radial force component of the suspension line force, F_{RL}.

c. Increasing the number of suspension lines in the parachute. As the number of lines is raised the tangent force in the canopy cloth at the main seam is used more efficiently and improves the inflation characteristics of the canopy.

3. For impermeable cloths (k=0), the critical velocity is infinite and the parachute always inflates.

4. For a value of n=0.5, the critical velocity is infinite.

5. As n approaches unity the ratio of the rate of cloth outflow per unit area to canopy mouth inflow rate per unit area is raised.

6. Test velocity affects the ratio of cloth rate of outflow per unit area to canopy mouth inflow rate per unit area. This is the key to critical velocity. All other observations are effects which modify the onset of critical velocity. The mass flow rate ratio, M', theoretically describes these effects. Increasing the test velocity raises the ratio of canopy outflow rate to inflow rate.

7. Triangular solid cloth parachute gores increase in local area from vent to canopy skirt hem. Even though the canopy cloth has a uniform rate of airflow (CFM/FT^2) the local canopy rate of airflow (CFM) is minimum through the cloth in the vent area and a maximum through the cloth in the skirt hem area. The total rate of airflow is PxS_o (CFM).

8. An increase in a solid cloth flat parachute's diameter generates 2.41 FT^2 of additional outflow area at the skirt hem for each 1 FT^2 of generated mouth inflow area. The additional area occurs at the canopy skirt hem where the flow rate is a maximum and most sensitive.

9. The effective canopy mouth area is reduced as the rate of airflow increases through the cloth or grid.

10. The canopy internal static pressure is reduced as the canopy rate of outflow is raised. The zone of higher than ambient static pressures extends ahead of the canopy skirt hem and diminishes as the distance ahead of the skirt hem increases.

11. As velocity increases, the parachute aerodynamic drag force increases. The collapsing component of the drag force, F_{RL}, in the suspension line is also increasing while the opposing inflationary force, F_{AC}, is decreasing due to the increase in the canopy rate of outflow to rate of inflow ratio. At the critical velocity, the rate of outflow exceeds the rate of inflow and the force, F_{RL}, causes the canopy to collapse until the inflow to outflow balance is re-established by the reduction of available outflow cloth area.

12. Once a parachute has squidded, a new force is introduced into the system. This squidding force is developed from the new deflected airflow pattern about the canopy which tends to stabilize the squidded parachute.

13. In order to overcome the squidding force, the velocity must be reduced below the squidding velocity.

14. The known phenomena that affect parachute criticality have been theoretically separately demonstrated.

15. A unified system that would calculate the critical velocity of a particular system from its design characteristics of suspension line length, number of suspension lines and the canopy type and rate of airflow has not been completed.

REFERENCES

1. Ludtke, W.P., A Summary of Parachute Technology Development at the Naval Surface Warfare Center, WO, NAVSWC TR 90-002, Section VII.

2. Ludtke, W.P., Observations on the Inflation Time and Inflation Distance of Parachutes, NAVSWC TR 88-292.

3. Ludtke, W.P., Notes on a Generic Parachute Opening Force Analysis, NAVSWC TR 86-142.

NOMENCLATURE

$2\bar{a}$ - Maximum steady-state inflated parachute diameter of gore mainseam, FT

A_M - Instantaneous canopy mouth area, FT^2

A_{ME} - Effective mouth area, FT^2

A_{MO} - Steady-state inflated mouth area, FT^2

A_s - Instantaneous pressurized canopy surface area during inflation, $A_s = S$ FT^2

A_{so} - Canopy surface area, FT^2
See S_o

$$A_{so} = S_o = \pi D_o^2/4$$

b - Minor axis of the steady-state inflated shape ellipse bounded by the major axis ($2\bar{a}$) and the vent of the canopy, FT

b' - Minor axis of the steady-state inflated shape ellipse which includes the skirt hem of the canopy, FT

C - Width of the unbillowed gore at the point of analysis

C' - Theoretical billowed gore circumference for minimum cloth stress

C_D - Parachute coefficient of drag

$C_D S_o$ - Parachute steady-state drag area, FT^2

C_{pav} - Parachute average pressure coefficient. The ratio of the instantaneous or steady-state drag force to the dynamic pressure times the parachute projected area.

d_{mo} - Steady-state mouth diameter of the inflated canopy, measured at the junction of the gore mainseam and the suspension lines at the canopy skirt hem, FT

D_o - Nominal diameter of the aerodynamic decelerator = $\sqrt{4S_o/\pi}$, FT

NOMENCLATURE (Cont.)

$2f$ - Inflated parachute chord line between two adjacent load lines at the point X_N, Y_N, β_N

F_{CA} - Aerodynamic force generated by the parachute canopy at the parachute skirt hem which tends to inflate the canopy, LBS.

F_{RL} - Suspension line radial force component at the parachute skirt hem which tends to collapse the canopy, LBS.

F_s - Steady-state drag force that would be produced by a fully open parachute at velocity V_s, LBS.

F_{SQ} - Side force which surrounds a squidded parachute and is directed toward the canopy centerline. The force, which is generated by redirection of the flow around the canopy, stabilizes the squidded parachute and delays canopy reinflation, LBS.

F_1 - Parachute suspension-line force, LBS

g - Gravitational acceleration, FT/SEC^2

k - Permeability constant of canopy cloth

L_e - Effective suspension line length. $L_e = L_s$ when the lines are connected at a single point

L_R - Length of a riser used to extend parachute suspension lines

L_s - Suspension line length

$\dot{m}_p$ - In the development of the derived inflation time equation $\dot{m}_p$ refers to the mass of air flowing

M - Ballistic Mass Ratio - ratio of the mass of the retarded hardware (including parachute) to a mass of atmosphere contained in a right circular cylinder of length ($V_s t_o$), face area ($C_D S_o$), and density (ρ)

NOMENCLATURE (Cont.)

M' - Mass flow rate ratio - ratio of the rate of atmosphere flowing through a unit of pressurized cloth area to the atmosphere flowing through a unit inlet area at arbitrary pressure. In some reports M' was termed the mass flow ratio.

n - Permeability constant of canopy cloth

N - Canopy depth is the distance from the skirt hem of the canopy to the vent of the canopy along the parachute center line

P - Cloth permeability - rate of airflow through a cloth at an arbitrary differential pressure CFM/FT^2 Military specifications specify a flow rate measured under a pressure differential of 1/2 inch of water

ΔP_{av} - Pressure differential acting on the inflated canopy projected area, PSF

q - Dynamic pressure, LB/FT^2

q_s - Steady-state dynamic pressure, LB/FT^2

r - Billowed gore radius of curvature

r' - Billowed gore radius of curvature for minimum stress

R - Canopy radius along the gore centerline

R_{at} - Ratio of the surface area of a ring of canopy cloth to the surface area of the first ring

R_{mo} - Mouth radius of the steady-state canopy=$d_{mo}/2$

R_o - $D_o/2$

S - Instantaneous pressurized canopy surface area $S=A_s$

NOMENCLATURE (Cont.)

t - Instantaneous time, SEC

t_o - Reference time when the parachute has reached the design drag area for the first time, SEC

V - Instantaneous system velocity, FT/SEC

V_{cr} - Parachute critical velocity, FT/SEC

V_o - Volume of air which must be collected during the inflation process, FT^3

V_s - Trajectory velocity at parachute line stretch, FT/SEC

W - System weight, LB

Z - Number of gores in the parachute

GREEK SYMBOLS

β - Semi-vetex angle between the suspension lines and the parachute center line and tangent to the transient pressurized canopy area during canopy inflation or the pseudo hem of a critically collapsed parachute , DEGREES.

β_o - Semi-vertex angle between the suspension lines and the parachute center line and tangent to the mainseam canopy hem, DEGREES

θ - Central angle subtended by the billowed gore, DEGREES

θ' - Central angle subtended by the billowed gore for minimum stress, DEGREES

ρ - Air density, $SLUGS/FT^3$

ρ_o - Sea level air density, $SLUGS/FT^3$

ϕ - Angle between the load line normal force and the force tangent to the canopy cloth at the load line, DEGREES

GREEK SYMBOLS (Cont.)

ψ - Angle subtended by a parachute gore in the plane of the canopy mouth = $180^{o}/Z$; also the unbillowed gore vertex angle, DEGREES

ψ' - Angle subtended by a parachute gore in the plane perpendicular to the load line at the point X_N, Y_N, β_N, DEGREES

DISTRIBUTION

	Copies
Commander Naval Air Systems Command Attn: Library	4
AIR-931H(F.Terry Thomasson) Technology Manager Crew Station & Life Support Systems(JP#1-Rm 424)	2
Department of the Navy Washington, DC 20361	
Commander Naval Sea Systems Command Attn: Library	4
Washington, DC 20362	
Commanding Officer Naval Personnel Research and Development Center Attn: Library	2
Washington, DC 20007	
Office of Naval Research Attn: Library	4
Washington, DC 20360	
Office of Naval Research Attn: Fluid Dynamics Branch	2
Structural Mechanics Branch	2
800 N. Quincy St. Arlington, VA 22217	
Commanding Officer Naval Ordnance Station Attn: Library	3
Christopher O'Donnell, (C ode 5920L)	6
Indian Head, MD 20640	

	Copies
Director Naval Research Laboratory Attn: Code 2027	
Library, Code 2029(ONRL)	2
Washington, DC 20375	
U.S. Naval Academy Attn: Library	2
Annapolis, MD 21402	
Superintendent U.S. Naval Postgraduate School Attn: Library (Code 0384)	2
Monterey, CA 93940	
Commander Naval Air Development Center Attn: Library	2
Dr. Norman Warner	1
Dr. Donald McErlean	1
Kenneth Greene	1
William B. Shope	1
David N. DeSimone	1
Louis A. Daulerio	1
Thomas J. Popp	1
Maria C. Hura	1
Warminster, PA 18974	
Commanding Officer Naval Weapons Support Center Attn: Library	2
Mark T. Little	1
Crane, IN 47522	
Commanding Officer Naval Weapons Center Attn: Library	2
Eric Smith	1
China Lake, CA 93555-6001	

DISTRIBUTION (Cont.)

	Copies
Commander Naval Ship Research and Development Center Attn: Library Washington, DC 20007	2
Commander Pacific Missile Test Center Attn: Technical Library, Code N0322 Point Mugu, CA 93041	2
Director Marine Corps Development and Education Command Development Center Attn: Library Quantico, VA 22134	2
Marine Corps Liaison Officer U.S. Army Natick Laboratories Natick, MA 01760	2
Commanding General U.S. Army Mobility Equipment Research and Development Center Attn: Technical Document Center Fort Belvoir, VA 22660	2
Commanding General U.S. Army Munitions Command Attn: Technical Library Stanley D. Kahn Dover, NJ 07801	2 1
Commanding General U.S. Army Weapons Command Attn: Technical Library Research and Development Directorate Rock Island, IL 61201	2
Commanding General U.S. Army ARDEC Attn: Library Walt Koenig, SMCAR-AET-A Roy W. Kline SMCAR-AET-A Dover, NJ 07801	2 1 1
Army Research and Development Laboratories Aberdeen Proving Ground Attn: Technical Library, Bldg. 313 Aberdeen, MD 21005	2
Commanding General Edgewood Arsenal Headquarters Attn: Library Aero Research Group Aberdeen Proving Ground Aberdeen, MD 21005	2
Commanding General Harry Diamond Laboratories Attn: Technical Library 2800 Powder Mill Road Adelphi, MD 20783	2

DISTRIBUTION (Cont.)

	Copies
U.S. Army Ballistic Research Laboratories Attn: Technical Library Aberdeen Proving Ground Aberdeen, MD 21005	2
Commanding General U.S. Army Foreign Science and Technology Center Attn: Technical Library 220 Seventh Street, NE Federal Building Charlottesville, VA 22312	
Commanding General U.S. Army Material Command Attn: Library Washington, DC 20315	2
Commanding General U.S. Army Test and Evaluation Command Attn: Library Aberdeen Proving Ground Aberdeen, MD 21005	2
Commanding General U.S. Army Combat Developments Command Attn: Library Fort Belvoir, VA 22060	2
Commanding General U.S. Army Combat Developments Command Attn: Technical Library Carlisle Barracks, PA 17013	2
Commanding General U.S. Army Material Laboratories Attn: Technical Library Fort Eustis, VA 23604	2
U.S. Army Air Mobility R&D Laboratory Eustis Directorate Attn: Systems and Equipment Division Fort Eustis, VA 23604	2
President U.S. Army Airborne Communications and Electronic Board Fort Bragg, NC 28307	2
Commanding General U.S. Missile Command Redstone Scientific Information Center Attn: Library Redstone Arsenal, AL 358091	2
Commander U.S. Army Natick R&D Labs Attn: Library James E. Sadek Peter Maske Calvin K. Lee M. P. Gionfriddo Joseph Gardella Timothy E. Dowling John Calligeros Carl Callianno DRDNA-UAS Kansis Street Natick, MA 01760-5017	2 1 1 1 1 1 1 1 1 1

DISTRIBUTION (Cont.)

	Copies
Commander U.S. Army Aviation Systems Command Attn: Library St. Louis, MO 63166	2
Office of the Chief of Research and Development Department of the Army Attn: Library Washington, DC 20315	2
U.S. Army Advanced Material Concepts Agency Department of the Army Attn: Library	2
Director U.S. Army Mobility R&D AMES Research Center Attn: Library Moffett Field, CA 94035	2
Commandant Quartermaster School Airborne Department Attn: Library Norman Bruneau Fort Lee VA 23801	2 2
U.S. Army Standardization Group, UK Attn: Research/General Material Representative Box 65 FPO, NY 09510	2
Commanding Officer McCallan AFB Attn: Library SA-ALC/MMIR McCallan AFB, CA 95652	2
Commanding Officer Wright-Patterson AFB Attn: William Casey ASD/ENECA William Pinnel, AFWAL/FIER Robert L. Hesters Jr. ASD/YYEE E. Schultz AFWAL/FIER Daniel J. Kolega Bldg. 25 Area B Patrick J. O'Brian Bldg. 25 Area B H. Engel ASD/ENECA A. Kididis ASD/ENECA OH 45433	1 1 1 1 1 1 1 1 1
Commanding Officer Air Force Flight Tests Center Attn: Airframe Systems Division Aerodynamic Decelerator Branch John A. Hed Edwards AFB, CA 93523	2 1
Commanding Officer Air Force Space Division Attn: Library P.O. Box 92960 Worldway Postal Center Los Angeles, CA 90009	2
Commanding Officer Air Force Aerophysics Laboratory Attn: Library Hanscom Field, MA	2
Command Officer Kelly AFB Attn: SA-ALC/MMIR Library TX 78241	2 2

DISTRIBUTION (Cont.)

	Copies
Arnold Engineering Development Center (ARO, Inc)	
Attn: Library/Documents	2
Arnold Air Force Station, TN 37389	
NASA Lewis Research Center	
Attn: Library, Mail Stop 60-3	2
21000 Brookpark Road	
Cleveland, OH 44135	
NASA John F. Kennedy Space Center	
Attn: Library, Code IS-CAS-42B	2
Kennedy Space Center, FL 32899	
NASA Manned Spacecraft Center	
Attn: Library, Code BM6	2
2101 Webster Seabrook Road	
Houston, TX 77058	
NASA Marshall Space Flight Center	
Attn: Library	2
Gary W. Johnson	1
Mail Code PT21	
Huntsville, AL 25812	
NASA Goddard Space Flight Center	
Wallops Island Flight Facility	
Attn: Library	2
Mr. Mendle Silbert	2
Mr. Earl B. Jackson	1
Mr. Dave Moltedo	1
Mr. Anel Flores	1
Mr. Phil Eberspeak	1
Wallops Island, VA 23337	
National Aeronautics and Space Administration	
Attn: Library	2
Headquarters, MTG	
400 Maryland Avenue, SW	
Washington, DC 20456	

	Copies
NASA Langley Research Center	
Langley Station	
Attn: Research Program Recording Unit, Mail Stop 122	1
Raymond L. Zavasky, Mail Stop 177	1
Andrew S. Wright, Jr. Mail Stop 401	8
George M. Warr	1
Hampton, VA 23365	
NASA Ames Research Center	
Attn: Library, Stop 202-3	2
Mr. Jim Ross	1
Moffett Field, CA 94035	
NASA Flight Research Center	
Attn: Library	2
P.O. Box 273	
Edwards, CA 93523	
NASA Goddard Space Flight Center	
Attn: Library	2
Greenbelt, MD 20771	
Jet Propulsion Laboratory	
Attn: Library, Mail 111-113	2
4800 Oak Grove Drive	
Pasadena, CA 91103	
NASA Johnson Space Center	
Attn: Library	2
Max Engert, Code EA	2
Joe Gamble, Mail Code 1A13	2
Kirby Hinson, Mail Code ET13	2
Houston, TX 77058	

DISTRIBUTION (Cont.)

	Copies
Defense Advanced Research Projects Agency Attn: Technical Library 1400 Wilson Boulevard Arlington, VA 22209	2
Director Defense Research and Engineering Attn: Library (Technical) The Pentagon Washington, DC 20301	2
Director of Defense Research and Engineering Department of Defense Washington, DC 20315	2
Defense Technical Information Center Cameron Station Alexandria, VA 22314	12
Library of Congress Attn: Gift and Exchange Division Washington, DC 20540	4
University of Minnesota Depart. of Aerospace Engineering Attn: Dr. W. L. Garrard Minneapolis, MN 55455	2
Center for Naval Analysis Attn: Technical Reference Library P.O. Box 16268 Arlington, VA 22302-0268	2
Sandia National Laboratories Attn: Code 1632	2
Library	2
Dr. Dean Wolf	1
Dr. Carl Peterson	10
R. Kurt Baca	1
Ira T. Holt	1
Donald W. Johnson	1
James W. Purvis	1
Harold E. Widdows	1
James Strickland	1
Don McBride	1
J. Michael Macha	1
Albuquerque, NM 87185	
Applied Physics Laboratory The Johns Hopkins University Attn: Document Librarian Johns Hopkins Road Laurel, MD 20810	2
National Academy of Sciences National Research Council Committee on Undersea Warfare Attn: Library 2101 Constitution Ave., N.W. Washington, DC 20418	2
Sandia Corporation Livermore Laboratory Attn: Technical Reference Library P.O. Box 969 Livermore, CA 9455	2
Lockheed Missiles and Space Co. Attn: Mr. K. French P.O. Box 504 Sunnyvale, CA 94086	1

DISTRIBUTION (Cont.)

	Copies	Copies
Rockwell International Corporation Space and Information Systems Div. Attn: Technical Information Center 12214 S. Lakewood Boulevard Downey, CA 90241	2	
Pennsylvania State University Applied Research Laboratory Attn: Library P.O. Box 30 State College, PA 16801	2	
Honeywell, Inc. Attn: RA Rausch (MN48-3700) 7225 Northland Drive Brooklyn Pk, MN 55428	1	
National Bureau of Standards Attn: Library Washington, DC 20234		
Internal distribution:		
U (H.D. Smith)	1	
U06 (J. Goeller)	1	
U13 (W. Parsons)	1	
U13 (W. P. Ludtke)	150	
U13 (D. Fiske)	1	
U13 (J. F. McNelia)	1	
U13 (J.Murphy)	1	
U13 (J. Correll)	1	
U13 (S.M. Hunter)	1	
U13 (R.L. Pense)	1	
U13 (M. L. Lama)	1	
U43 (J. Rosenberg)	1	
E231	2	
E232	3	
E31 (GIDEP)	1	
C72W	1	

REPORT DOCUMENTATION PAGE

Form Approved
OMB No. 0704-0188

1. AGENCY USE ONLY *(Leave blank)*	2. REPORT DATE	3. REPORT TYPE AND DATES COVERED
	25 June 1991	FY90 to FY91

4. TITLE AND SUBTITLE

Notes on the Cause of Parachute Critical Velocity

5. FUNDING NUMBERS

1U91CT

6. AUTHOR(S)

William P. Ludtke

7. PERFORMING ORGANIZATION NAME(S) AND ADDRESS(ES)

Naval Surface Warfare Center (U13)
10901 New Hampshire Avenue
Silver Spring, MD 20903-5000

8. PERFORMING ORGANIZATION REPORT NUMBER

9. SPONSORING/MONITORING AGENCY NAME(S) AND ADDRESS(ES)

10. SPONSORING/MONITORING AGENCY REPORT NUMBER

11. SUPPLEMENTARY NOTES

12a. DISTRIBUTION/AVAILABILITY STATEMENT

Approved for public release; distribution is unlimited.

12b. DISTRIBUTION CODE

13. ABSTRACT *(Maximum 200 words)*

This report discusses how the critical velocity of parachutes depends upon the rate of outflow through the canopy surface and the rate of inflow through the canopy mouth. The analysis indicates that the mass flow rate ratio, M', is demonstrated to be the theoretical key to the critical velocity of parachutes. All other observed effects modify the onset of critical velocity. The effects of M' and altitude on inflation reference time, parachute stability, drag coefficient, and inflation rate are also discussed.

14. SUBJECT TERMS

Parachute Technology
Critical Velocity
Number of Canopy Gores
Cloth Rate of Airflow
Suspension Line Length
Canopy Diameter

15. NUMBER OF PAGES

63

16. PRICE CODE

17. SECURITY CLASSIFICATION OF REPORT	18. SECURITY CLASSIFICATION OF THIS PAGE	19. SECURITY CLASSIFICATION OF ABSTRACT	20. LIMITATION OF ABSTRACT
Unclassified	Unclassified	Unclassified	SAR

GENERAL INSTRUCTIONS FOR COMPLETING SF 298

The Report Documentation Page (RDP) is used in announcing and cataloging reports. It is important that this information be consistent with the rest of the report, particularly the cover and its title page. Instructions for filling in each block of the form follow. It is important to ***stay within the lines*** to meet ***optical scanning requirements***.

Block 1. Agency Use Only *(Leave blank)*.

Block 2. Report Date. Full publication date including day, month, and year, if available (e.g. 1 Jan 88). Must cite at least the year.

Block 3. Type of Report and Dates Covered. State whether report is interim, final, etc. If applicable, enter inclusive report dates (e.g. 10 Jun 87 - 30 Jun 88).

Block 4. Title and Subtitle. A title is taken from the part of the report that provides the most meaningful and complete information. When a report is prepared in more than one volume, repeat the primary title, add volume number, and include subtitle for the specific volume. On classified documents enter the title classification in parentheses.

Block 5. Funding Numbers. To include contract and grant numbers; may include program element number(s), project number(s), task number(s), and work unit number(s). Use the following labels:

C	- Contract	**PR**	- Project
G	- Grant	**TA**	- Task
PE	- Program Element	**WU**	- Work Unit Accession No.

BLOCK 6. Author(s). Name(s) of person(s) responsible for writing the report, performing the research, or credited with the content of the report. *If editor or compiler, this should follow the name(s).*

Block 7. Performing Organization Name(s) and Address(es). Self-explanatory.

Block 8. Performing Organization Report Number. Enter the unique alphanumeric report number(s) assigned by the organization performing the report.

Block 9. Sponsoring/Monitoring Agency Name(s) and Address(es). Self-explanatory.

Block 10. Sponsoring/Monitoring Agency Report Number. *(If Known)*

Block 11. Supplementary Notes. Enter information not included elsewhere such as: Prepared in cooperation with...; Trans. of...; To be published in.... *When a report is revised, include a statement whether the new report supersedes or supplements the older report.*

Block 12a. Distribution/Availability Statement. Denotes public availability or limitations. Cite any availability to the public. Enter additional limitations or special markings in all capitals (e.g. NOFORN, REL, ITAR).

DOD	- See DoDD 5230.24, "Distribution Statements on Technical Documents."
DOE	- See authorities.
NASA	- See Handbook NHB 2200.2
NTIS	- Leave blank.

Block 12b. Distribution Code.

DOD	- Leave blank.
DOE	- Enter DOE distribution categories from the Standard Distribution for Unclassified Scientific and Technical Reports.
NASA	- Leave blank.
NTIS	- Leave blank.

Block 13. Abstract. Include a brief ***(Maximum 200 words)*** factual summary of the most significant information contained in the report.

Block 14. Subject Terms. Keywords or phrases identifying major subjects in the report.

Block 15. Number of Pages. Enter the total number of pages.

Block 16. Price Code. Enter appropriate price code ***(NTIS only)***

Blocks 17.-19. Security Classifications. Self-explanatory. Enter U.S. Security Classification in accordance with U.S. Security Regulations (i.e., UNCLASSIFIED). If form contains classified information, stamp classification on the top and bottom of the page.

Block 20. Limitation of Abstract. This block must be completed to assign a limitation to the abstract. Enter either UL (unlimited) or SAR (same as report). *An entry in this block is necessary if the abstract is to be limited.* If blank, the abstract is assumed to be unlimited.